(a)

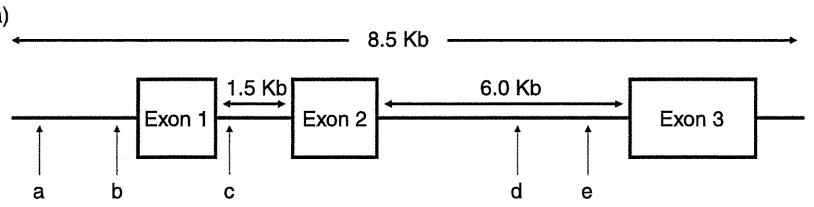

RANTES haplotype	a	b	c	d	e	Haplotype frequency
	rs2107538	rs2280788	rs2280789	rs4796120	rs3817655	
R1	G	C	T	A	A	0.599
R2	A	C	C	G	T	0.197
R3	A	G	C	A	T	0.189

(b)

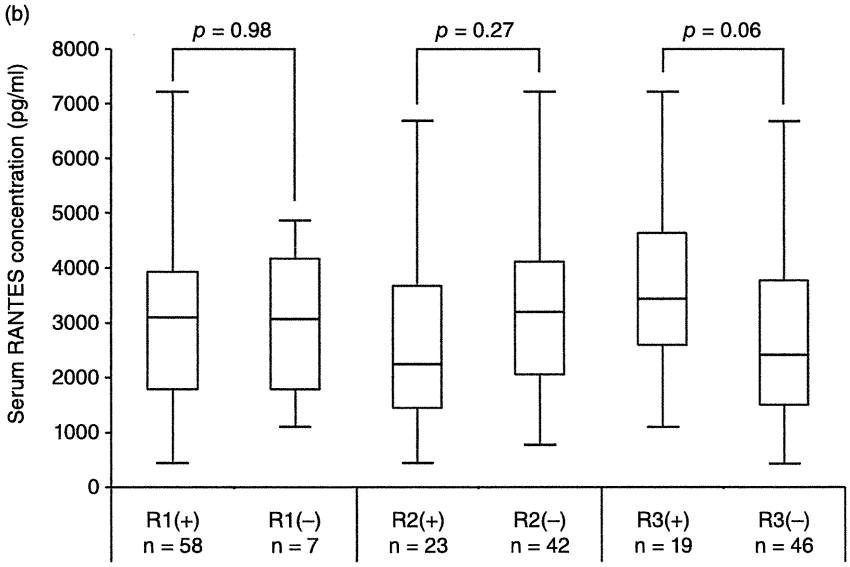

Figure 2 *RANTES* haplotypes and serum *RANTES* level. (a) *RANTES* haplotypes in the patients studied. The human *RANTES* gene spans 8.5 kb on chromosome 17q11-q12 and has the characteristic three exon and two intron organization of the CC chemokine family.[22] Exons are shown as open boxes while introns are shown as solid lines. Five single nucleotide polymorphisms (SNP) (rs2107538/rs2280788/rs2280789/rs4796120/rs3817655) were selected on the basis of data from the HapMap project (http://snp.cshl.org) to obtain complete coverage of the *RANTES* gene in the Japanese population. The locations of SNP variants are indicated by arrows. After the analysis of five *RANTES* SNP in 65 hepatitis C virus patients, haplotypes were determined using SNPAlyze software ver. 8.0 (Dynacom, Chiba, Japan) and divided into three groups on the basis of linkage disequilibrium. These were designated R1, R2 and R3 on the basis of haplotype frequency. (b) Serum *RANTES* level and *RANTES* haplotype. The correlation between serum the *RANTES* level and *RANTES* haplotype was investigated. Box and whisker plots shows distributions of serum *RANTES* levels for the haplotypes R1(+), R1(−), R2(+), R2(−), R3(+) and R3(−). The boxes represent the 25th to 75th percentile and horizontal lines within the boxes show the median values. The ends of the whiskers show the minimum and maximum values of all the data. *P*-values were obtained using Mann–Whitney's *U*-test. R1(+), the patients with the R1 haplotype; R1(−), the patients with a non-R1 haplotype; R2(+), the patients with the R2 haplotype; R2(−), the patients with a non-R2 haplotype; R3(+), the patients with the R3 haplotype; R3(−), the patients with a non-R3 haplotype.

further clarify the correlation. On the other hand, we could not show an association of pretreatment cytokines/chemokine concentrations with the treatment response to PEG IFN/RBV therapy for the other 35 cytokine and chemokine species investigated in this study. Recently, the serum level of *IP-10* was reported to be strongly associated with the response to PEG IFN/RBV therapy and baseline *IP-10* levels were elevated in patients infected with HCV genotype 1 or 4 who did not achieve an SVR after completion of interferon therapy.[19,20] In our study, however, *IP-10* was not extracted as a molecule associated with treatment responses. Actually, due to the measurement limit of the ELISA kit used, several cytokines and chemokines, including *IP-10*, were undetectable in this study, as shown in Table 2, raising the possibility that some cytokines and chemokines associated with SVR were not extracted. Therefore, our study cannot exclude the possibility of other cytokine/chemokines making a contribution to treatment efficacy.

In conclusion, we found that a high pretreatment serum *RANTES* level was related to the efficacy of PEG IFN/RBV therapy in genotype 1b HCV, independent of other treatment-restricting factors, and prediction of treatment outcome could be improved with the measurement of the pretreatment serum *RANTES* level.

ACKNOWLEDGMENTS

THIS WORK WAS supported by Grants-in-Aid from the Scientific Research Fund of the Ministry of Education, Science, Sports and Culture (21590836, 21590837, 23390195); and a Grant-in-Aid from the Ministry of Health, Labor and Welfare of Japan (H22-kanen-006).

REFERENCES

1 Kiyosawa K, Sodeyama T, Tanaka E *et al.* Interrelationship of blood transfusion, non-A, non-B hepatitis and hepatocellular carcinoma: analysis by detection of antibody to hepatitis C virus. *Hepatology* 1990; **12**: 671–5.
2 Singal AK, Singh A, Jaganmohan S *et al.* Antiviral therapy reduces risk of hepatocellular carcinoma in patients with hepatitis C virus-related cirrhosis. *Clin Gastroenterol Hepatol* 2010; **8**: 192–9.
3 Jacobson IM, McHutchison JG, Dusheiko G *et al.* Telaprevir for previously untreated chronic hepatitis C virus infection. *N Engl J Med* 2011; **364**: 2405–16.
4 Zeuzem S, Andreone P, Pol S *et al.* Telaprevir for retreatment of HCV infection. *N Engl J Med* 2011; **364**: 2417–28.
5 Fried MW. The role of triple therapy in HCV genotype 1-experienced patients. *Liver Int* 2011; **31** (Suppl 1): 58–61.
6 Akuta N, Suzuki F, Sezaki H *et al.* Association of amino acid substitution pattern in core protein of hepatitis C virus genotype 1b high viral load and non-virological response to interferon-ribavirin combination therapy. *Intervirology* 2005; **48**: 372–80.
7 Enomoto N, Sakuma I, Asahina Y *et al.* Mutations in the nonstructural protein 5A gene and response to interferon in patients with chronic hepatitis C virus 1b infection. *N Engl J Med* 1996; **334**: 77–81.
8 Conjeevaram HS, Kleiner DE, Everhart JE *et al.* Race, insulin resistance and hepatic steatosis in chronic hepatitis C. *Hepatology* 2007; **45**: 80–7.
9 Hickman IJ, Powell EE, Prins JB *et al.* In overweight patients with chronic hepatitis C, circulating insulin is associated with hepatic fibrosis: implications for therapy. *J Hepatol* 2003; **39**: 1042–8.
10 Shiffman ML, Mihas AA, Millwala F *et al.* Treatment of chronic hepatitis C virus in African Americans with genotypes 2 and 3. *Am J Gastroenterol* 2007; **102**: 761–6.
11 Shiffman ML, Suter F, Bacon BR *et al.* Peginterferon alfa-2a and ribavirin for 16 or 24 weeks in HCV genotype 2 or 3. *N Engl J Med* 2007; **357**: 124–34.
12 Suppiah V, Moldovan M, Ahlenstiel G *et al.* IL28B is associated with response to chronic hepatitis C interferon-alpha and ribavirin therapy. *Nat Genet* 2009; **41**: 1100–4.
13 Tanaka Y, Nishida N, Sugiyama M *et al.* Genome-wide association of IL28B with response to pegylated interferon-alpha and ribavirin therapy for chronic hepatitis C. *Nat Genet* 2009; **41**: 1105–9.
14 Katsounas A, Schlaak JF, Lempicki RA. CCL5: a double-edged sword in host defense against the hepatitis C virus. *Int Rev Immunol* 2011; **30**: 366–78.
15 Li K, Li NL, Wei D, Pfeffer SR, Fan M, Pfeffer LM. Activation of chemokine and inflammatory cytokine response in hepatitis C virus-infected hepatocytes depends on Toll-like receptor 3 sensing of hepatitis C virus double-stranded RNA intermediates. *Hepatology* 2012; **55**: 666–75.
16 Yoneda S, Umemura T, Joshita S *et al.* Serum chemokine levels are associated with the outcome of pegylated interferon and ribavirin therapy in patients with chronic hepatitis C. *Hepatol Res* 2011; **41**: 587–93.
17 Polyak SJ, Khabar KS, Rezeiq M, Gretch DR. Elevated levels of interleukin-8 in serum are associated with hepatitis C virus infection and resistance to interferon therapy. *J Virol* 2001; **75**: 6209–11.
18 Yee LJ, Tang J, Gibson AW, Kimberly R, Van Leeuwen DJ, Kaslow RA. Interleukin 10 polymorphisms as predictors of sustained response in antiviral therapy for chronic hepatitis C infection. *Hepatology* 2001; **33**: 708–12.
19 Butera D, Marukian S, Iwamaye AE *et al.* Plasma chemokine levels correlate with the outcome of antiviral therapy in patients with hepatitis C. *Blood* 2005; **106**: 1175–82.

20 Romero AI, Lagging M, Westin J *et al.* Interferon (IFN)-gamma-inducible protein-10: association with histological results, viral kinetics, and outcome during treatment with pegylated IFN-alpha 2a and ribavirin for chronic hepatitis C virus infection. *J Infect Dis* 2006; **194**: 895–903.
21 Kumada H, Okanoue T, Onji M *et al.* Guidelines for the treatment of chronic hepatitis and cirrhosis due to hepatitis C virus infection for the fiscal year 2008 in Japan. *Hepatol Res* 2010; **40**: 8–13.
22 Nelson PJ, Kim HT, Manning WC, Goralski TJ, Krensky AM. Genomic organization and transcriptional regulation of the RANTES chemokine gene. *J Immunol* 1993; **151**: 2601–12.
23 Schall TJ, Jongstra J, Dyer BJ *et al.* A human T cell-specific molecule is a member of a new gene family. *J Immunol* 1988; **141**: 1018–25.
24 Zlotnik A, Yoshie O. Chemokines: a new classification system and their role in immunity. *Immunity* 2000; **12**: 121–7.
25 Nattermann J, Nischalke HD, Feldmann G, Ahlenstiel G, Sauerbruch T, Spengler U. Binding of HCV E2 to CD81 induces RANTES secretion and internalization of CC chemokine receptor 5. *J Viral Hepat* 2004; **11**: 519–26.
26 Kaukinen P, Sillanpaa M, Kotenko S *et al.* Hepatitis C virus NS2 and NS3/4A proteins are potent inhibitors of host cell cytokine/chemokine gene expression. *Virol J* 2006; **3**: 66.
27 Ruggieri A, Franco M, Gatto I, Kumar A, Rapicetta M. Modulation of RANTES expression by HCV core protein in liver derived cell lines. *BMC Gastroenterol* 2007; **7**: 21.
28 Jang Y, Chae JS, Hyun YJ *et al.* The RANTES −403G > A promoter polymorphism in Korean men: association with serum RANTES concentration and coronary artery disease. *Clin Sci (Lond)* 2007; **113**: 349–56.
29 Zhernakova A, Alizadeh BZ, Eerligh P *et al.* Genetic variants of RANTES are associated with serum RANTES level and protection for type 1 diabetes. *Genes Immun* 2006; **7**: 544–9.
30 Promrat K, McDermott DH, Gonzalez CM *et al.* Associations of chemokine system polymorphisms with clinical outcomes and treatment responses of chronic hepatitis C. *Gastroenterology* 2003; **124**: 352–60.

Tetrahedron 69 (2013) 10884–10892

Contents lists available at ScienceDirect

Tetrahedron

journal homepage: www.elsevier.com/locate/tet

Synthesis of novel 4′-*C*-methyl-1′,3′-dioxolane pyrimidine nucleosides and evaluation of its anti-HIV-1 activity

Yutaka Kubota [a], Yuri Kaneda [a], Kazuhiro Haraguchi [b,*], Mirei Mizuno [a], Hiroshi Abe [c], Satoshi Shuto [c], Takayuki Hamasaki [d], Masanori Baba [d], Hiromichi Tanaka [a]

[a] *School of Pharmacy, Showa University, 1-5-8 Hatanodai, Shinagawa-ku, Tokyo 142-8555, Japan*
[b] *Nihon Pharmaceutical University, 10281 Komuro, Inamachi, Kita-adachi-gun, Saitama 362-0806, Japan*
[c] *Faculty of Pharmaceutical Sciences, Hokkaido University, Kita-12, Nishi-6, Kita-ku, Sapporo 060-0812, Japan*
[d] *Division of Antiviral Chemotherapy, Center for Chronic Viral Diseases, Graduate School of Medical and Dental Sciences, Kagoshima University, Kagoshima 890-8544, Japan*

ARTICLE INFO

Article history:
Received 11 October 2013
Received in revised form 23 October 2013
Accepted 24 October 2013
Available online 30 October 2013

ABSTRACT

The key glycosyl donor for the target molecule **12** was prepared by two-step sequences; (1) acetalization of *tert*-butyldimethylsilyloxyacetaldehyde with 3-bromopropanediol, (2) DBN-initiated β-elimination of the resulting 2-(*tert*-butyldimethylsilyloxy)methyl-4-bromomethyl-1,3-dioxolane **11**. Electrophilic glycosidation between **12** and silylated pyrimidine nucleobase proceeded efficiently to provide a mixture of β- and α-anomers of the respective glycosides **14** and **15**. Tin radical-mediated reduction of the bromomethyl functional group of **14** and **15** gave protected 4′-*C*-methyl-dioxorane uracil- **16** and thymine nucleoside **17**. The respective cytosine nucleoside **18** was synthesized from **16**. De-silylation of 4′-methyl-1′,3′-dioxolane pyrimidine nucleosides **16**–**18** gave the target molecules. Evaluation of the anti-HIV-1 activity of the β- and α-anomers of the novel 4′-*C*-methyl-1′,3′-dioxolane nucleosides **22**β,α–**24**β,α revealed that none of the nucleoside derivatives possess anti-viral activity against HIV-1 and show cytotoxicity against MT-4 cells at 100 μM.

1. Introduction

Nucleoside analogues are recognized as an important class of biologically active compounds, especially as anti-viral and antitumor agents.[1–3] Among their sugar-modified analogues, 1′,3′-dioxolane nucleoside, in which the 3′-methylene moiety in the furanose ring of 2′,3′-dideoxynucleosides is replaced with an oxygen atom, have attracted much attention since the discovery of the moderate anti-HIV-1 activity of a racemic mixture of (−)-β-D- (**1**) and (+)-β-L-1′,3′-dioxolane thymine nucleoside (*ent*-**2**) in ATH8 cells in 1989 (Fig. 1).[4]

Asymmetric synthetic studies of 1′,3′-dioxolanyl thymine nucleoside revealed that the (−)-β-D-isomer **1** is more potent than the (+)-β-L-isomer *ent*-**2**.[5] Interestingly, the study pointed out that the racemic mixture of the thymine-dioxolane nucleosides was more potent than either the (−)-D-β-isomer or (+)-L-β-isomer because of the additive effects of both of the enantiomers. Also, another structure–activity relationship study demonstrated that the (−)-α-cytosine derivative **3** showed anti-viral activity although the potency of its activity is less than that of (+)-β-isomer **4**[6] (Fig. 2).

In 2001, the synthesis of 2′-*C*-methyl-1′,3′-dioxolanyl cytosine nucleosides **4** and **5**, as the first branched dioxolanyl nucleosides, was reported (Fig. 3).[7] In this study, anti-viral assays of **4**β,α and **5**β,α were carried out and none of these derivatives were found to show anti-HIV activity. Other examples of branched dioxolane nucleosides are the 5′-*C*-methyl-1′,3′-dioxolanylpurine nucleosides **6**–**8**, these have been synthesized and as in the case of 2′-branched derivatives, these nucleosides did not display significant anti-HIV activities[8] (Fig. 4).

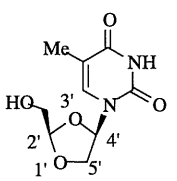

(−)-β-D-1′,3′-dioxolane-thymine nucleoside (**1**)

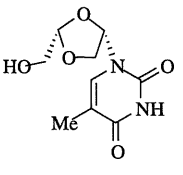

(+)-β-L-1′,3′-dioxolane-thymine nucleoside (**2**)

Fig. 1. Structures of compound **1** and *ent*-**2**.

* Corresponding author. Tel.: +81 48 721 1155; fax: +81 48 721 6208; e-mail address: harakazu@nichiyaku.ac.jp (K. Haraguchi).

0040-4020/$ – see front matter © 2013 Elsevier Ltd. All rights reserved.
http://dx.doi.org/10.1016/j.tet.2013.10.075

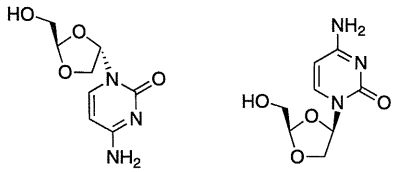

3α **3β**

Fig. 2. Structures of (−)-α-D-**3α** and (+)-β-D-1′,3′-dioxolanyl cytosine nucleosides **3β**.

4β: β-D-isomer (X = cytosin-1-yl, Y = H)
4α: α-D-isomer (X = H, Y = cytosin-1-yl)

5β: α-L-isomer (X = cytosin-1-yl, Y = H)
5α: β-L-isomer (X = H, Y = cytosin-1-yl)

Fig. 3. Structures of 2′-*C*-methyl-1′,3′-dioxolanyl cytosine nucleosides **4**β,α and **5**β,α.

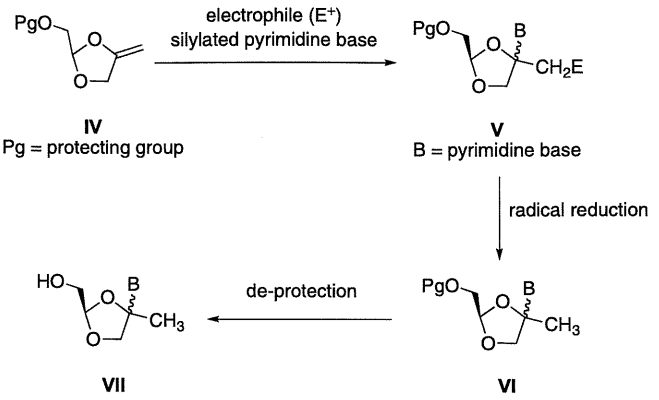

Scheme 1. Synthetic plan for the target molecules **VII**.

mediated reductive removal of the E group in **V** and deprotection of the resulting **VI** would furnish the target 4′-*C*-methyl-1′,3′-dioxolane pyrimidine nucleosides **VII**.

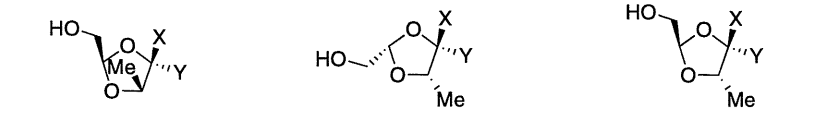

6β: X = adenin-9-yl or guanin-9-yl; Y = H
6α: X = H; Y = adenin-9-yl or guanin-9-yl

7β: X = adenin-9-yl or guanin-9-yl; Y = H
7α: X = H; Y = adenin-9-yl or guanin-9-yl

8β: X = guanin-9-yl; Y = H
8α: X = H; Y = guanin-9-yl

Fig. 4. Structures of 5′-*C*-methyl-1′,3′-dioxolanyl nucleosides **6**–**8**.

In this context, as an extension of structure–activity relationships for methyl-branched dioxolanyl nucleosides, we have been interested in the synthesis and evaluation of the anti-HIV activities of the β- and α-anomers of novel 4′-*C*-methyl branched nucleosides, such as uracil **I**, thymine **II**, and cytosine nucleoside **III** (Fig. 5) because nucleoside analogues branched at the anomeric position with a methyl group possess interesting biological activities.[9,10] In this paper, we will describe the detailed results of this study.

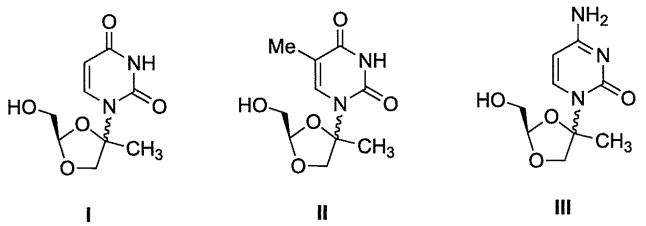

I **II** **III**

Fig. 5. Structures of the target 4′-*C*-methyl-1′,3′-dioxolanyl pyrimidine nucleosides **I**–**III**.

2. Results

2.1. Chemistry

Our synthetic plan for the target molecules is outlined in Scheme 1. Thus, 4-exomethylene 1,3-dioxolane **IV** was selected as the key glycosyl donor for the target nucleosides **I**–**III**. Electrophilic glycosidation between **IV** and silylated pyrimidine base would provide the respective glycosides **V**. Subsequently, tin radical-

Initially, the preparation of exomethylene 1,3-dioxolane **IV** was examined. Thus, *tert*-butyldimethylsilyloxy(TBSO)acetaldehyde **9** was reacted with 3-bromopropanediol **10** in the presence of *p*-toluenesulfonic acid in benzene under reflux conditions to give the cyclic acetal, 2-TBSO-methyl-4-bromomethyl-1,3-dioxolane **11** in 71% yield (Scheme 2). For the preparation of the key glycosyl donor **12**, **11** was subjected to a base-mediated elimination reaction (Scheme 3). When **11** was reacted with potassium *tert*-butoxide in CH_3CN under reflux conditions, the desired **12** could not be obtained and lead to the formation of a mixture of unidentified products. In contrast, the desired elimination reaction proceeded

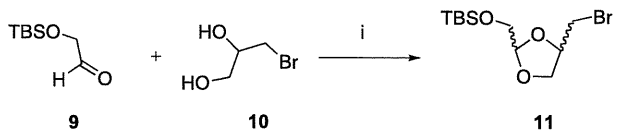

9 **10** **11**

Scheme 2. Synthesis of 4-bromomethyl-2-TBSO-methyl-1,3-dioxolane **11**. Reactions and conditions: (i) *p*-TsOH·H_2O, benzene, reflux; **11** (71%).

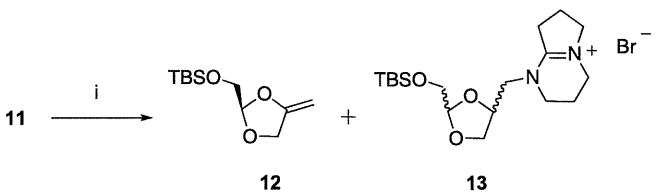

12 **13**

Scheme 3. Elimination of **11**: formation of exomethylene 1,3-dioxolane **12** and substitution product **13**. Reactions and conditions: (i) DBN, CH_3CN, reflux; **12** (30%), **13** (67%).

using DBN as the base to provide **12** in 30% yield although the substituted product **13** was also formed in 67% yield. The enol ether **12** was found to decompose during silica gel column chromatography. Due to this instability to acidic media, the purification of **12** was performed using neutral alumina. At the present time, the isolated yield of **12** could not be improved.

With the glycosyl donor **12** in hand, electrophilic glycosidation with silylated uracil was examined (Scheme 4). When **12** was reacted with bis-*O*-trimethylsilyl(TMS)uracil (3.0 equiv) in the presence of *N*-iodosuccinimide (NIS) (1.1 equiv) in CH_2Cl_2 for 0.5 h, a mixture of the stereoisomers of the target glycosides **14** was formed. After HPLC separation, β-anomer **14**β and α-anomer **14**α could be obtained in 39% and 46% isolated yields, respectively. The stereochemistry of the respective isomers was assigned on the basis of NOE experimental results as follows; **14**β: H-6/CH_2OTBS (3.9%), **14**α: H-6/H-2′α (3.4%).

Table 1
Glycosidation between **12** and silylated uracil by changing the solvent[a]

Entry	Solvent	Combined yield (%)	Ratio of **14**β/**14**α[b]
1	CH_2Cl_2	85	1:1.2
2	CH_3CN	84	1:1.7
3	$ClCH_2CH_2Cl$	82	1:1.1
4	CCl_4	81	1:1.5
5	THF	80	1:1.1
6	Benzene	67	1:1.3
7	Toluene	81	1:1.3

[a] All reactions were carried out by using NIS (1.1 equiv) and silylated uracil (3.0 equiv) at rt in the solvent indicated.
[b] The ratio was determined by integrating the respective H-6.

respectively (Scheme 5). Likewise, the α-isomers **14**α and **15**α could be transformed into **16**α and **17**α in 97% and 98% yields, respectively (Fig. 7).

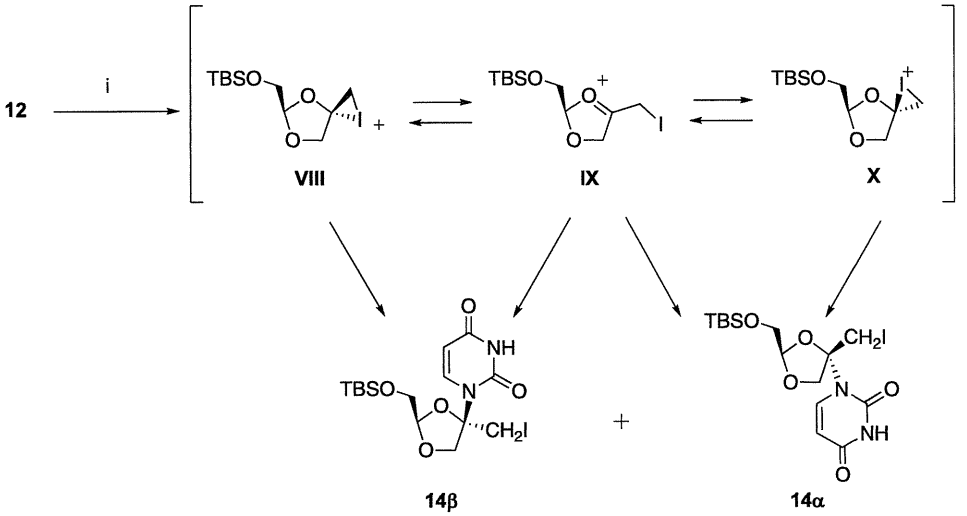

Scheme 4. Electrophilic glycosidation between **12** and silylated uracil to lead to 1′,3′-dioxolane uracil nucleosides **14**β and **14**α. Reactions and conditions: (i) bis-*O*-TMS-uracil (3.0 equiv), *N*-iodosuccinimide (1.1 equiv), CH_2Cl_2; **14**β (39%) and **14**α (46%).

In this glycosidation reaction, the reaction intermediates are the α-iodonium ion **VIII**, β-iodonium ion **X**, and oxonium ion **IX** and the subsequent nucleophilic addition of silylated uracil to the iodonium ions **VIII** and **X** give the β-anomer **14**β and α-anomer **14**α respectively, whereas the oxonium ion **IX** provides both of the anomers. Therefore, the isolated yields of **14**β and **14**α would be dependent upon the ratio of **VIII**–**X**. In the course of our ongoing research on the synthetic chemistry of unsaturated sugar nucleosides,[11] we have recently reported the iodo-benzoyloxylation of 3′,4′-unsaturated adenosine derivative utilizing NIS and benzoic acid.[12] In this study, the ratio of the *anti*- and *syn*-adducts was different when we compared the reactions of CH_2Cl_2 and THF. These results indicated that the ratio of iodonium and oxonium ions was influenced by solvent effects. This fact led us to carry out the glycosidation shown in Scheme 4 in various solvents. However, as shown in Table 1, significant solvent effects were not observed in the solvents (CH_3CN, $ClCH_2CH_2Cl$, CCl_4, THF, benzene, and toluene) examined.

In the same manner utilized for the preparation of uracil nucleosides, the thymine glycosides **15**β and **15**α could be obtained in 34% and 44% yields, respectively, using bis-*O*-TMS-thymine (Fig. 6). The stereochemistry of the products was also determined by NOE data; **15**β: H-6/CH_2OTBS (3.9%), **15**α: H-6/H-2′α (3.5%).

Next, the β-anomers **14**β and **15**β were subjected to tin radical-mediated reduction to give 4′-*C*-methyl-1′,3′-dioxolanyl nucleosides **16**β (isolated yield; 97%) and **17**β (isolated yield; 98%),

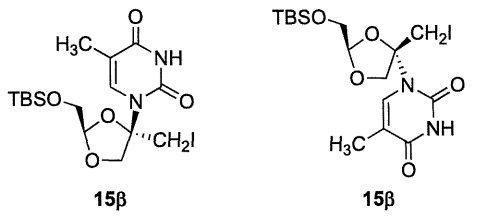

Fig. 6. Structure of 1,3-dioxolane thymine nucleosides **15**β and **15**α.

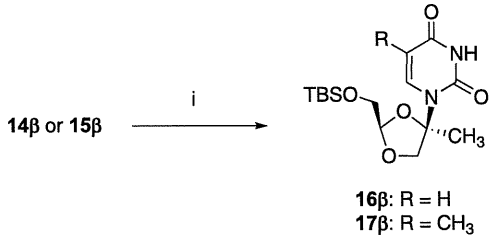

Scheme 5. Radical reduction of the β-anomers of glycosidated products **14**β and **15**β: formation of **16**β and **17**β. Reactions and conditions: (i) Bu_3SnH, AIBN, benzene; **16**β (97%), **17**β (98%).

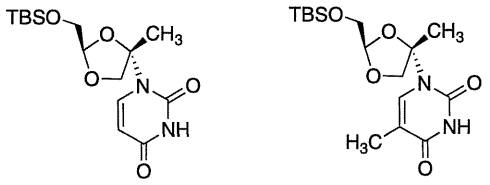

Fig. 7. Structures of α-anomers of 4′-methyl-1′,3′-dioxolane nucleosides **16**α and **17**α.

For synthesizing cytosine nucleosides, **16**β and **16**α were reacted with 2,4,6-triisopropylbenzenesulfonyl chloride and the resulting 4-*O*-sulfonate was subsequently treated with ammonium hydroxide to give **18**β and **18**α in 62% and 68% isolated yields, respectively, for two steps (Scheme 6).

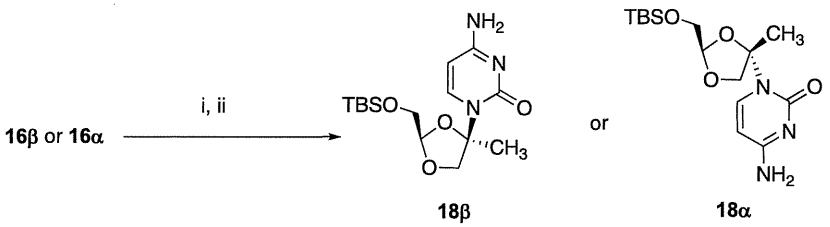

Scheme 6. Synthesis of 1′,3′-dioxolane cytosine nucleoside **18**β and **18**α. Reactions and conditions: (i) 2,4,6-triisopropylbenzenesulfonyl chloride, Et_3N, CH_3CN, 60 °C, 4 h; (ii) NH_4OH/THF, 0 °C to rt, 13 h; **18**β (78%), **18**α (68%).

Finally, **16**β–**18**β were converted into the title compounds 4′-*C*-methyl-1′,3′-dioxolanyl nucleosides **22**β–**24**β through desilylative-acetylation and subsequent deacetylation sequences (Scheme 7). In the same manner, the α-isomers **22**α–**24**α could also be obtained (Fig. 8).

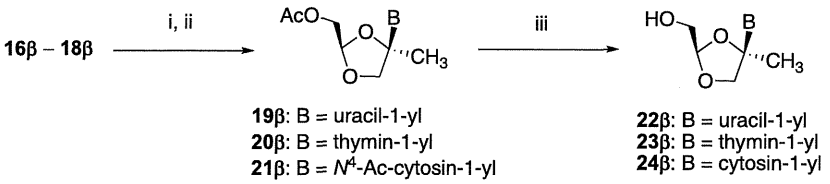

Scheme 7. Synthesis of β-anomers of 4′-methyl-1′,3′-dioxolane pyrimidine nucleosides **22**β–**24**β through its acetates **19**β–**21**β. Reactions and conditions: (i) Bu_4NF, THF, rt, 1 h; (ii) Ac_2O, rt, 16 h; **19**β (52%), **20**β (80%), **21**β (90%) (two steps); (iii) Et_3N, MeOH, rt, 6 h; **22**β (95%), **23**β (96%), **24**β (94%).

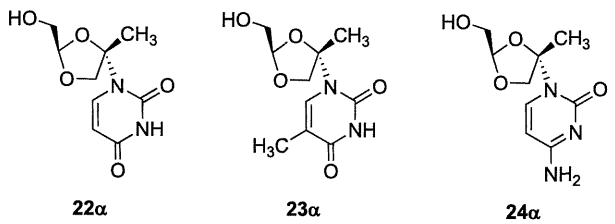

Fig. 8. Structures of α-anomers of 4′-methyl-1′,3′-dioxolane pyrimidine nucleosides **22**α–**24**α.

2.2. Theoretical calculations

In order to examine the influence of the 4′-methyl substituent on the puckering of the dioxolane moiety, molecular orbital calculations were performed to determine the relative energies of northern- and southern-type conformers of **1** and **23**β (Table 1). The north conformer and south conformer were defined as 42° or −42° in dihedral angle C4′–C5′–O1′–C2′. Rotational energies of the glycosidated bonds O3′–C4′–N1′–C6 were calculated in the north or south conformers, respectively, at the HF/3-21G* level using the Gaussian 09 program 20. The unsubstituted dioxolane thymine nucleoside **1** adopted the northern-*anti* puckering as a preferential conformation, which is consisted with the X-ray crystallographic analysis.[4] As can be seen in Fig. 9, introduction of a methyl substituent at the 4′-positon has been found to have no influence on the conformation of the dioxolane ring, which has the same preferential puckering. However, in the case of methyl-substituted **23**β, the energy level of the north-*syn* conformer of **23**β was found to be larger than that of the unsubstituted **1**.

2.3. Anti-HIV evaluation

The novel nucleoside derivatives **22**β–**24**β and **22**α–**24**α synthesized in this study were evaluated against HIV-1 in MT-4 cells.[13,14] None of the described compounds showed activity against HIV-1 and cytotoxicity against MT-4 cells in this assay at 100 μM.

3. Conclusion

In this study, we have demonstrated the synthesis of novel 1′,3′-dioxolane pyrimidine nucleosides branched at the 4′-position with a methyl group. The key glycosidated donor **12** could be easily prepared from *tert*-butyldimethylsilyloxyacetaldehyde and 3-bromopropanediol in two steps. The electrophilic glycosidation between **12** and silylated pyrimidine bases proceeded efficiently to provide the respective β- and α-anomers in nearly equal amounts in excellent isolated yields. Although the glycosidation was carried out in several polar and non-polar solvents, no solvent effect for the ratio of the stereoisomers was observed.

It was anticipated that the introduction of a 4′-methyl group might impose a conformational preference distinct from that of

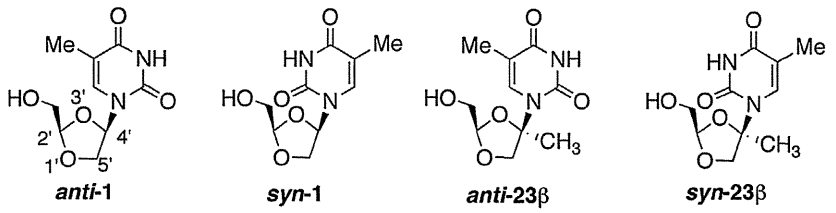

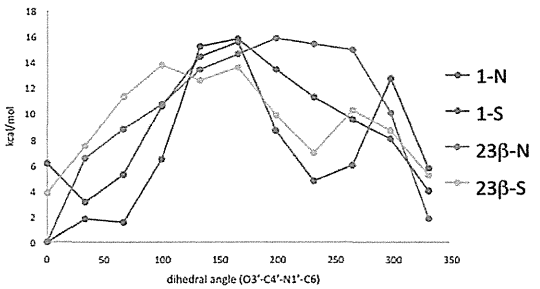

1-N: North conformer of **1**; **1**-S: South conformer of **1**
23β-N: North conformer of **23**β; **23**β-S: South conformer of **23**β

Fig. 9. Relative energies in kcal/mol of canonical conformations of **1** and **23**β, calculated by molecular mechanics.

the unsubstituted **1**. Therefore, molecular mechanics calculations were carried out to assess the influence of the introduction of the 4′-methyl substituent on conformational preference. Our calculations predicted that **23**β adopts a similar puckering (northern-*anti*) to that of **1**, suggesting that the substitution at the 4′-position does not alter the sugar puckering of the parent dioxolane T.

The novel nucleoside analogues synthesized in this study were evaluated against HIV-1 in vitro. Despite the fact that 1′,3′-dioxolane thymine and cytosine nucleosides possess anti-HIV activity, none of the 4′-methyl-substituted derivatives displayed any antiviral activity. It has been reported that *syn*- and *anti*-conformer play critical role for the binding of nucleoside ligands to an enzyme.[15] Thus, 6,5′-cyclo- and 6,3′-methanouridines exemplified as *anti*-fixed isomers did not bind to uridine phophorylase whereas the binding affinities of *syn*-fixed 2,2′-anhydro- and 2,5′-anhydrouridine increased. This fact caused us to speculate that the instability of *syn*-conformer of **23**β, which would play important role for the recognition by kinases, could be responsible for the observed inactivity against HIV-1.

4. Methods

4.1. General methods

Melting points are uncorrected. ^{1}H and ^{13}C NMR spectra were recorded either at 400 MHz or at 500 MHz. Chemical shifts are reported relative to Me_4Si. Mass spectra (MS) were taken in FAB mode with *m*-nitrobenzyl alcohol as a matrix. Column chromatography was carried out on silica gel. Thin-layer chromatography (TLC) was performed on silica gel. When necessary, analytical samples were purified by high performance liquid chromatography (HPLC), which was carried out on a Shimadzu LC-6AD with a Shimpack PREP-SIL (H) KIT column (2×25 cm). THF was distilled from benzophenone ketyl.

4.2. *cis*- and *trans*-4-Bromomethyl-2-(*tert*-butyldimethylsilyloxy)methyl-1,3-dioxolane (11)

To a solution of *tert*-butyldimethylsilyloxyacetaldehyde **9**[16] (3.2 mL, 15 mmol) and 3-bromo-1,2-propanediol **10**[17] (1.6 mL, 18 mmol) in benzene (50 mL) was added *para*-toluenesulfonic acid monohydrate (285 mg, 1.5 mmol) and the reaction mixture was stirred for 14 h at reflux temperature using Dean–Stark apparatus. The reaction mixture was quenched with $NaHCO_3$, diluted with EtOAc, and washed with saturated $NaHCO_3$/saturated NaCl. Silica gel column chromatography (hexane/ethyl acetate=30:1) of the organic layer gave **11** (3.3 g, 71%) as a colorless liquid: ^{1}H NMR ($CDCl_3$) δ 0.08 and 0.09 (6H, each as s, Si–Me), 0.90 and 0.91 (9H, each as s, Si–*tert*-Bu), 3.23–3.36 (1H, m, CH_{2a}Br-4), 3.45 (1H, dd, $J_{4,4\text{-}CH2aBr}$=4.9 Hz and $J_{4\text{-}CH2a,4\text{-}CH2b}$=10.0 Hz, CH_{2b}Br-4), 3.64–3.71 (2H, m, CH_2OTBS-2), 3.79 (1H, dd, $J_{4,5a}$=5.6 Hz and $J_{5a,5b}$=8.3 Hz, H-5a), 4.22 (1H, dd, $J_{4,5b}$=8.5 Hz and $J_{5a,5b}$=8.3 Hz, H-5b), 4.32–4.36 (1H, m, H-4), 5.03–5.16 (1H, m, H-2); ^{13}C NMR ($CDCl_3$) δ −5.4, 18.3, 18.4, 25.8, 25.8, 31.9, 32.1, 64.4, 64.6, 69.0, 69.4, 75.3, 75.4, 104.7, 105.1; FABMS (*m*/*z*) 311 (M^++H). FAB-HRMS (*m*/*z*): calcd for $C_{11}H_{23}BrO_3Si$: 311.0678, found: 311.0571 (M^++H).

4.3. 2-(*tert*-Butyldimethylsilyloxy)methyl-4-methylidene-1,3-diolorane (12) and *cis*- and *trans*-2-(*tert*-butyldimethylsilyloxy)methyl-4-(1,5-diazabicyclo[4.3.0]nonenium) bromide (13)

To a solution of **11** (100 mg, 0.32 mmol) in CH_3CN (5 mL) was added DBN (0.2 mL, 1.5 mmol) at 0 °C and the reaction mixture was stirred for 3 h at reflux temperature. The reaction mixture was diluted with EtOAc and washed with saturated NH_4Cl/saturated NaCl. The organic layer was dried (Na_2SO_4) and evaporated to dryness. The residue was diluted with hexane/ethyl acetate and filtered through a neutral alumina pad. The filtrate was evaporated to dryness to give **12** (22 mg, 30%, liquid). The alumina pad was

washed with CH_2Cl_2/MeOH (10:1) to give **13** (93 mg, 67%, pale yellow liquid).

4.3.1. Physical data of ***12****.* ^{1}H NMR ($CDCl_3$) δ 0.08 and 0.09 (6H, each as s, Si–Me), 0.90 (9H, each as s, Si–*tert*-Bu), 3.74 (2H, d, $J_{2,CH2OTBS}$=3.6 Hz, CH_2OTBS-2), 3.90 (1H, ddd, $J_{4\text{-}CH2a,5a}$=1.7 Hz and $J_{4\text{-}CH2a,5b}$=3.2 Hz and $J_{4\text{-}CH2a,4\text{-}CH2b}$=2.2 Hz, CH_{2a}-4), 4.35 (1H, ddd, $J_{4\text{-}CH2b,5a}$=2.0 Hz, $J_{4\text{-}CH2b,5b}$=2.2 Hz and $J_{4\text{-}CH2a,4\text{-}CH2b}$=2.2 Hz, CH_{2b}-4), 4.42 (1H, ddd, $J_{4\text{-}CH2a,5a}$=1.7 Hz, $J_{4\text{-}CH2b,5a}$=2.0 Hz and $J_{5a,5b}$=12.0 Hz, H-5a), 4.55 (1H, ddd, $J_{4\text{-}CH2a,5b}$=3.2 Hz, $J_{4\text{-}CH2b,5b}$=2.2 Hz and $J_{5a,5b}$=12.0 Hz, H-5b), 5.33 (1H, t, $J_{2,CH2aOTBS}$=$J_{2,CH2bOTBS}$=3.6 Hz, H-2); ^{13}C NMR ($CDCl_3$) δ −5.4, 18.4, 29.7, 64.4, 67.3, 76.7, 106.2, 156.0; FABMS (*m*/*z*) 231 (M^++H). FAB-HRMS (*m*/*z*): calcd for $C_{11}H_{22}O_3Si$: 231.1416, found: 231.1417 (M^++H).

4.3.2. Physical data of ***13****.* ^{1}H NMR ($CDCl_3$) δ 0.03 and 0.05 (6H, each as s, Si–Me), 0.85 and 0.86 (9H, each as s, Si–*tert*-Bu), 3.29–3.68 (14H, m, CH_2-4′, CH_2-2, CH_2-3, CH_2-4, CH_2-7, CH_2-8 and CH_2-9), 3.90–4.09 (2H, m, CH_2-5′), 4.35–4.41 (1H, m, H-4′), 4.91 and 5.06 (1H, each as t, $J_{2',CH2OTBS}$=3.4 Hz, H-2′); ^{13}C NMR ($CDCl_3$) δ −5.2, −5.1, −3.0, 18.0, 18.2, 18.2, 18.8, 25.9, 25.9, 26.0, 30.5, 42.1, 45.3, 45.4, 54.2, 54.3, 55.1, 64.0, 64.1, 67.0, 67.1, 73.5, 73.7, 103.2, 104.3, 164.9, 164.9, 170.2; FABMS (*m*/*z*) 355 (M^++H). FAB-HRMS (*m*/*z*): calcd for $C_{18}H_{35}N_2O_3Si$: 355.2417, found: 355.2350 (M^++H).

4.4. *r*-2-(*tert*-Butyldimethylsilyloxy)methyl-*t*-4-iodomethyl-*c*-4-(uracil-1-yl)-1,3-dioxolane (14β) and *r*-2-(*tert*-butyldimethylsilyloxy)methyl-*c*-4-iodomethyl-*t*-4-(uracil-1-yl)-1,3-dioxolane (14α)

To a solution of **12** (50.0 mg, 0.22 mmol) in CH_2Cl_2 (1.5 mL) were added bis-*O*-TMS-uracil (166.7 mg, 0.65 mmol) and NIS (53.7 mg, 0.24 mmol) and the reaction mixture was stirred at rt under Ar atmosphere for 0.5 h. The reaction mixture was partitioned between CH_2Cl_2 and saturated $NaHCO_3$–saturated $Na_2S_2O_3$. Silica gel column chromatography (hexane/ethyl acetate=5:1) of the organic layer gave a mixture of **14**β and **14**α (92.5 mg, 85%, **14**β/**14**α=1:1.2) as a yellow foam, which was separated by HPLC (hexane/ethyl acetate=1:1) to give **14**β (t_R=5.0 min, 46.3 mg, 43%, foam) and **14**α (t_R=7.1 min, 46.3 mg, 43%, foam).

4.4.1. Physical data of ***14****β.* UV (MeOH) λ_{max} 261 nm (ε 12,300) and λ_{min} 233 nm (ε 4600); ^{1}H NMR ($CDCl_3$) δ 0.03 and 0.05 (6H, each as s, Si–Me), 0.86 (9H, s, Si–*tert*-Bu), 3.65 (1H, d, $J_{4'\text{-}CH2a,4'\text{-}CH2b}$=11.1 Hz, ICH_{2a}-4′), 3.78 (1H, dd, $J_{2',2'\text{-}TBSOCH2a}$=2.4 Hz and $J_{2'\text{-}TBSOCH2a,2'\text{-}TBSOCH2b}$=12.1 Hz, TBSO$CH_{2a}$-2′), 3.84 (1H, dd, $J_{2',2'\text{-}TBSOCH2b}$=2.4 Hz and $J_{2'\text{-}TBSOCH2a,2'\text{-}TBSOCH2b}$=12.1 Hz, TBSO$CH_{2b}$-2′), 4.11 (1H, d, $J_{4'\text{-}CH2a,4'\text{-}CH2b}$=11.1 Hz, ICH_{2b}-4′), 4.36 (1H, d, $J_{5'a,5'b}$=10.1 Hz, H-5′a), 4.81 (1H, d, $J_{5'a,5'b}$=10.1 Hz, H-5′b), 5.32 (1H, t, $J_{2',2'\text{-}TBSOCH2a}$=$J_{2',2'\text{-}TBSOCH2b}$=2.4 Hz, H-2′), 5.71 (1H, d, $J_{5,6}$=8.3 Hz, H-5), 7.86 (1H, d, $J_{5,6}$=8.3 Hz, H-6), 8.89 (1H, br, NH); NOE (500 MHz, $CDCl_3$): irradiated CH2a-I/observed H-2′(1.2%), irradiated TBSOCH$_2$-2′/observed H-6 (3.9%); ^{13}C NMR ($CDCl_3$) δ −5.6, −5.4, 9.7, 18.4, 25.7, 63.1, 74.0, 93.1, 100.7, 106.6, 141.3, 150.1, 163.7; FABMS (*m*/*z*) 469 (M^++H). Anal. Calcd for $C_{15}H_{25}IN_2O_5Si\cdot 7/8CH_3OH$: C, 38.38; H, 5.23; N, 5.69. Found: C, 38.02; H, 5.22; N, 5.69.

4.4.2. Physical data of ***14****α.* UV (MeOH) λ_{max} 261 nm (ε 10,700) and λ_{min} 231 nm (ε 2200); ^{1}H NMR ($CDCl_3$) δ 0.12 and 0.13 (6H, each as s, Si–Me), 0.92 (9H, s, Si–*tert*-Bu), 3.60 (1H, d, $J_{4'\text{-}CH2a,4'\text{-}CH2b}$=11.0 Hz, ICH_{2a}-4′), 3.84 (2H, d, $J_{2',2'\text{-}TBSOCH2}$=2.4 Hz, TBSOCH_2-2′), 4.11 (1H, d, $J_{4'\text{-}CH2a,4'\text{-}CH2b}$=11.0 Hz, ICH_{2b}-4′), 4.41 (1H, d, $J_{5'a,5'b}$=10.5 Hz, H-5′a), 4.64 (1H, d, $J_{5'a,5'b}$=10.1 Hz, H-5′b), 5.16 (1H, t, $J_{2',2'\text{-}TBSOCH2a}$=$J_{2',2'\text{-}TBSOCH2b}$=3.3 Hz, H-2′), 5.76 (1H, d, $J_{5,6}$=8.3 Hz, H-5), 7.69 (1H, d, $J_{5,6}$=8.3 Hz, H-6), 9.41 (1H, br, NH); NOE (500 MHz, $CDCl_3$): irradiated H-2′/observed H-6 (3.4%); ^{13}C NMR ($CDCl_3$) δ −5.3, 9.9, 18.4, 25.8, 63.5, 74.8, 93.1, 101.3, 105.5, 140.2, 150.2, 163.8; FABMS (*m*/*z*) 469 (M^++H). Anal. Calcd for $C_{15}H_{25}IN_2O_5Si\cdot 7/8CH_3OH$: C, 38.38; H, 5.23; N, 5.69. Found: C, 38.02; H, 5.22; N, 5.69.

4.5. *r*-2-(*tert*-Butyldimethylsilyloxy)methyl-*t*-4-iodomethyl-*c*-4-(thymin-1-yl)-1,3-dioxolane (15β) and *r*-2-(*tert*-butyldimethylsilyloxy)methyl-*c*-4-iodomethyl-*t*-4-(thymin-1-yl)-1,3-dioxolane (15α)

Compounds **15**β and **15**α were prepared as described above for **14** starting from bis-*O*-TMS-thymine (175.8 mg, 0.65 mmol), a solution of **12** (50 mg, 0.22 mmol) in CH_2Cl_2 (1.5 mL), and NIS (53.7 mg, 0.24 mmol). Silica gel column chromatography on silica gel (hexane/ethyl acetate=5:1) of the crude product mixture gave a mixture of **15**β and **15**α (81.3 mg, 78%, **15**β/**15**α=1:1.3). HPLC separation (hexane/ethyl acetate=2:1) gave analytically pure sample of **15**β (t_R=6.7 min, 35.3 mg, 34%) and **15**α (t_R=9.1 min, 46 mg, 44%).

4.5.1. Physical data of ***15****β.* UV (MeOH) λ_{max} 266 nm (ε 8600) and λ_{min} 236 nm (ε 2300); ^{1}H NMR ($CDCl_3$) δ 0.02 and 0.04 (6H, each as s, Si–Me), 0.86 (9H, s, Si–*tert*-Bu), 1.95 (3H, d, $J_{CH3,6}$=2.4 Hz, CH_3-5), 3.65 (1H, d, $J_{4'\text{-}CH2a,4'\text{-}CH2b}$=11.1 Hz, ICH_{2a}-4′), 3.76 (1H, dd, $J_{2',2'\text{-}TBSOCH2a}$=2.7 Hz and $J_{2'\text{-}TBSOCH2a,2'\text{-}TBSOCH2b}$=12.1 Hz, TBSO$CH_{2a}$-2′), 3.82 (1H, dd, $J_{2',2'\text{-}TBSOCH2b}$=2.4 Hz and $J_{2'\text{-}TBSOCH2a,2'\text{-}TBSOCH2b}$=12.1 Hz, TBSO$CH_{2b}$-2′), 4.07 (1H, d, $J_{4'\text{-}CH2a,4'\text{-}CH2b}$=11.1 Hz, ICH_{2b}-4′), 4.41 (1H, d, $J_{5'a,5'b}$=10.1 Hz, H-5′a), 4.78 (1H, d, $J_{5'a,5'b}$=10.1 Hz, H-5′b), 5.35 (1H, dd, $J_{2',2'\text{-}TBSOCH2a}$=2.7 Hz and $J_{2',2'\text{-}TBSOCH2b}$=2.4 Hz, H-2′), 7.64 (1H, d, $J_{CH3,6}$=1.2 Hz, H-6), 8.53 (1H, br, NH); NOE (500 MHz, $CDCl_3$): irradiated TBSOCH_2-2′/observed H-6 (3.9%); ^{13}C NMR ($CDCl_3$) δ −5.7, −5.5, 10.0, 18.2, 25.6, 63.4, 74.2, 92.9, 106.5, 109.0, 136.9, 150.3, 164.7; FABMS (*m*/*z*) 483 (M^++H). Anal. Calcd for $C_{16}H_{27}IN_2O_5Si$: C, 39.84; H, 5.64; N, 5.81. Found: C, 39.66; H, 5.77; N, 5.88.

4.5.2. Physical data of ***15****α.* UV (MeOH) λ_{max} 266 nm (ε 10,300) and λ_{min} 234 nm (ε 2500); ^{1}H NMR ($CDCl_3$) δ 0.10 and 0.12 (6H, each as s, Si–Me), 0.90 (9H, s, Si–*tert*-Bu), 1.93 (3H, d, $J_{CH3,6}$=1.1 Hz, CH_3-5), 2.97 (1H, d, $J_{4'\text{-}CH2a,4'\text{-}CH2b}$=11.0 Hz, ICH_{2a}-4′), 3.84 (2H, d, $J_{2',2'\text{-}TBSOCH2}$=3.4 Hz, TBSOCH_2-2′), 4.07 (1H, d, $J_{4'\text{-}CH2a,4'\text{-}CH2b}$=11.0 Hz, ICH_{2b}-4′), 4.37 (1H, d, $J_{5'a,5'b}$=10.0 Hz, H-5′a), 4.63 (1H, d, $J_{5'a,5'b}$=10.0 Hz, H-5′b), 5.13 (1H, t, $J_{2',2'\text{-}TBSOCH2a}$=$J_{2',2'\text{-}TBSOCH2b}$=3.3 Hz, H-2′), 7.50 (1H, d, $J_{CH3,6}$=1.1 Hz, H-6), 10.13 (1H, br, NH); NOE (500 MHz, $CDCl_3$): irradiated H-2′/observed H-6 (3.5%); ^{13}C NMR ($CDCl_3$) δ −5.3, 10.0, 12.6, 18.3, 25.8, 63.4, 75.0, 92.8, 105.3, 109.6, 135.8, 150.3, 164.7; FABMS (*m*/*z*) 483 (M^++H). Anal. Calcd for $C_{16}H_{27}IN_2O_5Si$: C, 39.84; H, 5.64; N, 5.81. Found: C, 40.08; H, 5.70; N, 5.51.

4.6. *r*-2-(*tert*-Butyldimethylsilyloxy)methyl-*t*-4-methyl-*c*-4-(uracil-1-yl)-1,3-dioxolane (16β)

To a solution of **14**β (522.6 mg, 1.12 mmol) in benzene (9.7 mL) were added tributyltin hydride (0.90 mL, 3.35 mmol) and AIBN (274.7 mg, 1.67 mmol) at rt under Ar atmosphere and the reaction mixture was stirred under reflux temperature for 1.0 h. Silica gel column chromatography (hexane/ethyl acetate=5:1) of the reaction mixture gave **16**β as a foam; UV (MeOH) λ_{max} 263 nm (ε 9600) and λ_{min} 231 nm (ε 1700); ^{1}H NMR ($CDCl_3$) δ 0.03 and 0.06 (6H, each as s, Si–Me), 0.87 (9H, s, Si–*tert*-Bu), 1.76 (3H, s, CH3-4′), 3.73 (1H, dd, $J_{2',2'\text{-}TBSOCH2a}$=3.2 Hz and $J_{2'\text{-}TBSOCH2a,2'\text{-}TBSOCH2b}$=11.7 Hz, TBSO$CH_{2a}$-2′), 3.78 (1H, dd, $J_{2',2'\text{-}TBSOCH2b}$=2.9 Hz and $J_{2'\text{-}TBSOCH2a,2'\text{-}TBSOCH2b}$=11.7 Hz, TBSO$CH_{2b}$-2′), 3.99 (1H, d, $J_{5'a,5'b}$=10.0 Hz, H-5′a), 4.81 (1H, d, $J_{5'a,5'b}$=10.0 Hz, H-5′b), 5.19 (1H, dd, $J_{2',2'\text{-}TBSOCH2a}$=3.2 Hz and $J_{2',2'\text{-}TBSOCH2b}$=2.9 Hz, H-2′), 5.68 (1H,

d, $J_{5,6}$=8.3 Hz, H-5), 7.90 (1H, d, $J_{5,6}$=8.3 Hz, H-6), 9.19 (1H, br, NH); ^{13}C NMR ($CDCl_3$) δ −5.5, −5.4, 18.4, 23.9, 25.8, 63.2, 75.7, 94.3, 101.1, 105.7, 140.6, 150.2, 163.8; FABMS (*m*/*z*) 343 (M^++H). Anal. Calcd for $C_{15}H_{26}N_2O_5Si$: C, 52.61; H, 7.65; N, 8.18. Found: C, 52.65; H, 7.66; N, 8.05.

4.7. *r*-2-(*tert*-Butyldimethylsilyloxy)methyl-*t*-4-methyl-*c*-4-(thymin-1-yl)-1,3-dioxolane (17β)

Compound **17**β was prepared as described above for **16**β starting from a solution of **15**β (255.0 mg, 0.53 mmol) in benzene (5.0 mL), tributyltin hydride (0.42 mL, 1.59 mmol), and AIBN (130.0 mg, 0.79 mmol). Silica gel column chromatography (hexane/ethyl acetate=8:1) of the reaction mixture gave a mixture of **17**β (183.0 mg, 97%) as a foam: UV (MeOH) λ_{max} 267 nm (ε 9100) and λ_{min} 235 nm (ε 1800); ^{1}H NMR ($CDCl_3$) δ 0.03 and 0.06 (6H, each as s, Si–Me), 0.87 (9H, s, Si–*tert*-Bu), 1.72 (3H, s, CH_3-4′), 1.92 (3H, d, $J_{5\text{-}CH3,6}$=1.1 Hz, CH_3-5), 3.71 (1H, dd, $J_{2',2'\text{-TBSOCH2a}}$=3.4 Hz and $J_{2'\text{-TBSOCH2a},2'\text{-TBSOCH2b}}$=11.7 Hz, TBSO$CH_{2a}$-2′), 3.77 (1H, dd, $J_{2',2'\text{-TBSOCH2b}}$=3.0 Hz and $J_{2'\text{-TBSOCH2a},2'\text{-TBSOCH2b}}$=11.7 Hz, TBSO$CH_{2b}$-2′), 4.02 (1H, d, $J_{5'a,5'b}$=10.0 Hz, H-5′a), 4.78 (1H, d, $J_{5'a,5'b}$=10.0 Hz, H-5′b), 5.21 (1H, dd, $J_{2',2'\text{-TBSOCH2a}}$=3.4 Hz and $J_{2',2'\text{-TBSOCH2b}}$=3.0 Hz, H-2′), 7.67 (1H, d, $J_{5\text{-}CH3,6}$=1.1 Hz, H-6), 8.76 (1H, br, NH); ^{13}C NMR ($CDCl_3$) δ −5.5, −5.4, 12.7, 18.4, 24.0, 25.7, 63.6, 75.8, 94.1, 105.6, 109.5, 136.3, 150.0, 164.2; FABMS (*m*/*z*) 357 (M^++H). Anal. Calcd for $C_{16}H_{27}N_2O_5Si$: C, 53.91; H, 7.92; N, 7.86. Found: C, 54.12; H, 7.99; N, 7.55.

4.8. *r*-2-(*tert*-Butyldimethylsilyloxy)methyl-*c*-4-methyl-*t*-4-(uracil-1-yl)-1,3-dioxolane (16α)

Compound **16**α was prepared as described above for **16**β starting from a solution of **14**α (280.3 mg, 0.60 mmol) in benzene (5.2 mL), tributyltin hydride (0.52 mL, 1.79 mmol), and AIBN (147.3 mg, 0.90 mmol). Silica gel column chromatography (hexane/ethyl acetate=4:1) of the reaction mixture gave **16**α (148.2 mg, 72%) as a foam: UV (MeOH) λ_{max} 263 nm (ε 9900) and λ_{min} 231 nm (ε 1800); ^{1}H NMR ($CDCl_3$) δ 0.10 and 0.11 (6H, each as s, Si–Me), 0.91 (9H, s, Si–*tert*-Bu), 1.72 (3H, s, CH_3-4′), 3.77 (1H, dd, $J_{2',2'\text{-TBSOCH2a}}$=3.3 Hz and $J_{2'\text{-TBSOCH2a},2'\text{-TBSOCH2b}}$=11.7 Hz, TBSO$CH_{2a}$-2′), 3.80 (1H, dd, $J_{2',2'\text{-TBSOCH2b}}$=3.4 Hz and $J_{2'\text{-TBSOCH2a},2'\text{-TBSOCH2b}}$=11.7 Hz, TBSO$CH_{2b}$-2′), 4.32 (1H, d, $J_{5'a,5'b}$=10.0 Hz, H-5′a), 4.39 (1H, d, $J_{5'a,5'b}$=10.0 Hz, H-5′b), 5.08 (1H, dd, $J_{2',2'\text{-TBSOCH2a}}$=3.3 Hz and $J_{2',2'\text{-TBSOCH2b}}$=3.4 Hz, H-2′), 5.73 (1H, d, $J_{5,6}$=8.3 Hz, H-5), 7.72 (1H, d, $J_{5,6}$=8.3 Hz, H-6), 9.09 (1H, br, NH); ^{13}C NMR ($CDCl_3$) δ −5.3, 18.4, 24.2, 25.8, 63.9, 76.3, 94.8, 101.8, 104.8, 150.0, 163.2; FABMS (*m*/*z*) 343 (M^++H). Anal. Calcd for $C_{15}H_{26}N_2O_5Si$: C, 52.61; H, 7.65; N, 8.18. Found: C, 52.76; H, 7.67; N, 8.08.

4.9. *r*-2-(*tert*-Butyldimethylsilyloxy)methyl-*c*-4-methyl-*t*-4-(thymin-1-yl)-1,3-dioxolane (17α)

Compound **17**α was prepared as described above for **16**β starting from a solution of **15**α (462.0 mg, 0.96 mmol) in benzene (10.0 mL), tributyltin hydride (0.76 mL, 2.88 mmol), and AIBN (236.0 mg, 1.44 mmol). Silica gel column chromatography (hexane/ethyl acetate=7:1) of the reaction mixture gave **17**α (337.4 mg, 99%) as a foam: UV (MeOH) λ_{max} 268 nm (ε 9200) and λ_{min} 235 nm (ε 1700); ^{1}H NMR ($CDCl_3$) δ 0.10 and 0.11 (6H, each as s, Si–Me), 0.92 (9H, s, Si–*tert*-Bu), 1.72 (3H, s, CH_3-4′), 1.94 (3H, s, $J_{5\text{-}CH3,6}$=1.2 Hz, CH_3-5), 3.78 (1H, dd, $J_{2',2'\text{-TBSOCH2a}}$=3.4 Hz and $J_{2'\text{-TBSOCH2a},2'\text{-TBSOCH2b}}$=11.0 Hz, TBSO$CH_{2a}$-2′), 3.82 (1H, dd, $J_{2',2'\text{-TBSOCH2b}}$=3.4 Hz and $J_{2'\text{-TBSOCH2a},2'\text{-TBSOCH2b}}$=11.0 Hz, TBSO$CH_{2b}$-2′), 4.32 (1H, d, $J_{5'a,5'b}$=9.9 Hz, H-5′a), 4.37 (1H, d, $J_{5'a,5'b}$=9.9 Hz, H-5′b), 5.07 (1H, t, $J_{2',2'\text{-TBSOCH2a}}$=$J_{2',2'\text{-TBSOCH2b}}$=3.4 Hz, H-2′), 7.56 (1H, d, $J_{5\text{-}CH3,6}$=1.2 Hz, H-6), 8.63 (1H, br, NH); ^{13}C NMR ($CDCl_3$) δ −5.3, 12.7, 18.4, 24.3, 25.8, 63.8, 76.4, 94.4, 104.6, 110.2, 135.2, 150.1, 164.2; FABMS (*m*/*z*) 357 (M^++H). Anal. Calcd for $C_{16}H_{28}N_2O_5Si$: C, 53.91; H, 7.92; N, 7.86. Found: C, 53.59; H, 7.91; N, 7.61.

4.10. *r*-2-(*tert*-Butyldimethylsilyloxy)methyl-*t*-4-methyl-*c*-4-(cytosin-1-yl)-1,3-dioxolane (18β)

To a solution of **16**β (357.6 mg, 1.04 mmol) in CH_3CN (9.0 mL) were added 2,4,6-triisopropylbenzenesulfonyl chloride (632.5 mL, 2.09 mmol) and potassium carbonate (721.6 mg, 5.22 mmol) at rt under Ar atmosphere and the reaction mixture was stirred at 60 °C for 4.0 h. Silica gel column chromatography (dichloromethane/methanol=200:1) of the reaction mixture gave the respective 4-*O*-sulfonate. To a solution of the sulfonate in THF (46.0 mL) was added ammonium hydroxide at 0 °C and the reaction mixture was stirred at rt. The reaction mixture was partitioned between CH_2Cl_2/H_2O and silica gel column chromatography (dichloromethane/methanol=30:1) of the organic layer gave **18**β (277.4 mg, 78%) as a foam: UV (MeOH) λ_{max} 270 nm (ε 8000) and λ_{min} 233 nm (ε 5100); ^{1}H NMR ($CDCl_3$) δ −0.01 and 0.03 (6H, each as s, Si–Me), 0.85 (9H, s, Si–*tert*-Bu), 1.77 (3H, s, CH_3-4′), 3.66 (1H, dd, $J_{2',2'\text{-TBSOCH2a}}$=3.7 Hz and $J_{2'\text{-TBSOCH2a},2'\text{-TBSOCH2b}}$=11.5 Hz, TBSO$CH_{2a}$-2′), 3.71 (2H, dd, $J_{2',2'\text{-TBSOCH2b}}$=3.4 Hz and $J_{2'\text{-TBSOCH2a},2'\text{-TBSOCH2b}}$=11.5 Hz, TBSO$CH_{2b}$-2′), 4.04 (1H, d, $J_{5'a,5'b}$=10.0 Hz, H-5′a), 4.75 (1H, d, $J_{5'a,5'b}$=10.0 Hz, H-5′b), 5.18 (1H, dd, $J_{2',2'\text{-TBSOCH2a}}$=3.7 Hz and $J_{2',2'\text{-TBSOCH2b}}$=3.4 Hz, H-2′), 5.84 (1H, d, $J_{5,6}$=7.6 Hz, H-5), 7.89 (1H, d, $J_{5,6}$=7.6 Hz, H-6); ^{13}C NMR ($CDCl_3$) δ −5.5, −5.4, 18.3, 24.1, 25.8, 63.4, 75.7, 93.9, 94.2, 105.2, 141.5, 155.2, 165.6; FABMS (*m*/*z*) 342 (M^++H). Anal. Calcd for $C_{15}H_{27}N_3O_4Si\cdot 1/3H_2O$: C, 51.85; H, 8.02; N, 12.10. Found: C, 52.00; H, 7.89; N, 12.00.

4.11. *r*-2-(*tert*-Butyldimethylsilyloxy)methyl-*c*-4-methyl-*t*-4-(cytosin-1-yl)-1,3-dioxolane (18α)

To a solution of **16**α (639.7 mg, 1.87 mmol) in CH_3CN (17.0 mL) were added 2,4,6-triisopropylbenzenesulfonyl chloride (1.10 g, 3.74 mmol) and potassium carbonate (1.30 g, 9.34 mmol) at rt under Ar atmosphere and the reaction mixture was stirred at 60 °C for 4.0 h. Silica gel column chromatography (hexane/ethyl acetate=10:1) of the reaction mixture gave the respective 4-*O*-sulfonate. To a solution of the sulfonate in THF (63.0 mL) was added ammonium hydroxide (105 mL) at 0 °C and the reaction mixture was stirred at rt for 20 h. The reaction mixture was partitioned between CH_2Cl_2/H_2O and silica gel column chromatography (dichloromethane/methanol=25:1) of the organic layer gave **18**α (434.6 mg, 68%) as a foam: UV (MeOH) λ_{max} 272 nm (ε 7500) and λ_{min} 235 nm (ε 5700); ^{1}H NMR ($CDCl_3$) δ 0.10 and 0.11 (6H, each as s, Si–Me), 0.91 (9H, s, Si–*tert*-Bu), 1.75 (3H, s, CH_3-4′), 3.78 (1H, dd, $J_{2',2'\text{-TBSOCH2a}}$=3.4 Hz and $J_{2'\text{-TBSOCH2a},2'\text{-TBSOCH2b}}$=13.2 Hz, TBSO$CH_{2a}$-2′), 3.80 (1H, dd, $J_{2',2'\text{-TBSOCH2b}}$=3.4 Hz and $J_{2'\text{-TBSOCH2a},2'\text{-TBSOCH2b}}$=13.2 Hz, TBSO$CH_{2b}$-2′), 4.37 (1H, d, $J_{5'a,5'b}$=10.1 Hz, H-5′a), 4.42 (1H, d, $J_{5'a,5'b}$=10.1 Hz, H-5′b), 5.02 (1H, t, $J_{2',2'\text{-TBSOCH2a}}$=$J_{2',2'\text{-TBSOCH2b}}$=3.4 Hz, H-2′), 5.77 (1H, d, $J_{5,6}$=7.6 Hz, H-5), 7.83 (1H, d, $J_{5,6}$=7.6 Hz, H-6); ^{13}C NMR ($CDCl_3$) δ −5.3, 18.4, 24.6, 63.9, 94.4, 104.1, 140.2, 155.7, 165.1; FABMS (*m*/*z*) 342 (M^++H). Anal. Calcd for $C_{15}H_{27}N_3O_4Si\cdot 5/16H_2O$: C, 52.32; H, 8.10; N, 11.95. Found: C, 52.42; H, 7.97; N, 11.57.

4.12. *r*-2-Acetoxymethyl-*t*-4-methyl-*c*-4-(uracil-1-yl)-1,3-dioxolane (19β)

To a solution of **16**β (1.10 g, 3.21 mmol) in THF (93.0 mL) was added tetrabutylammonium fluoride (1 M THF solution) (4.8 mL, 4.82 mmol) at rt under Ar atmosphere and the reaction mixture was stirred for 2.0 h. To the reaction mixture was added Ac_2O (1.5 mL, 16.06 mmol) and the mixture was stirred for 14 h. The reaction mixture was partitioned between CH_2Cl_2/saturated $NaHCO_3$ and silica gel column chromatography (hexane/ethyl

acetate=1:2) of the organic layer gave **19**β (194.9 mg, 52%) as a foam; UV (MeOH) λ_{max} 261 nm (ε 9700) and λ_{min} 231 nm (ε 1900); ^{1}H NMR ($CDCl_3$) δ 1.75 (3H, s, CH_3-4′), 2.05 (3H, s, Ac), 3.99 (1H, d, $J_{5'a,5'b}$=10.2 Hz, H-5′a), 4.19 (1H, dd, $J_{2',2'\text{-TBSOCH2a}}$=3.2 Hz and $J_{2'\text{-TBSOCH2a},2'\text{-TBSOCH2b}}$=12.4 Hz, TBSO$CH_{2a}$-2′), 4.24 (1H, dd, $J_{2',2'\text{-TBSOCH2b}}$=3.2 Hz and $J_{2'\text{-TBSOCH2a},2'\text{-TBSOCH2b}}$=12.4 Hz, TBSO$CH_{2b}$-2′), 4.93 (1H, d, $J_{5'a,5'b}$=10.2 Hz, H-5′b), 5.35 (1H, t, $J_{2',2'\text{-TBSOCH2a}}$=$J_{2',2'\text{-TBSOCH2b}}$=3.2 Hz, H-2′), 5.75 (1H, d, $J_{5,6}$=8.3 Hz, H-5), 7.84 (1H, d, $J_{5,6}$=8.3 Hz, H-6), 9.96 (1H, br, NH); ^{13}C NMR ($CDCl_3$) δ 20.7, 23.6, 62.2, 75.4, 94.4, 101.3, 102.9, 140.0, 150.3, 164.1, 170.2; FABMS (*m*/*z*) 271 (M^++H). Anal. Calcd for $C_{11}H_{14}N_2O_6$: C, 48.89; H, 5.22; N, 10.37. Found: C, 48.62; H, 5.31; N, 10.06.

4.13. *r*-2-Acetoxymethyl-*t*-4-methyl-*c*-4-(thymin-1-yl)-1,3-dioxolane (20β)

To a solution of **17**β (183.2 mg, 0.51 mmol) in THF (15.0 mL) was added tetrabutylammonium fluoride (1 M THF solution) (0.8 mL, 0.77 mmol) at rt under Ar atmosphere and the reaction mixture was stirred for 2.0 h. To the reaction mixture was added Ac_2O (70 μL, 0.77 mmol) and the mixture was stirred for 16 h. The reaction mixture was partitioned between CH_2Cl_2/saturated $NaHCO_3$ and silica gel column chromatography (dichloromethane/methanol=100:1) of the organic layer gave **20**β (117.4 mg, 80%) as a foam: ^{1}H NMR ($CDCl_3$) δ 1.76 (3H, s, CH_3-4′), 1.96 (3H, s, $J_{CH3,6}$=1.1 Hz, CH_3-5), 2.07 (3H, s, Ac), 3.99 (1H, d, $J_{5'a,5'b}$=10.2 Hz, H-5′a), 4.19 (1H, dd, $J_{2',2'\text{-TBSOCH2a}}$=3.4 Hz and $J_{2'\text{-TBSOCH2a},2'\text{-TBSOCH2b}}$=12.3 Hz, TBSO$CH_{2a}$-2′), 4.37 (1H, dd, $J_{2',2'\text{-TBSOCH2b}}$=3.4 Hz and $J_{2'\text{-TBSOCH2a},2'\text{-TBSOCH2b}}$=12.3 Hz, TBSO$CH_{2b}$-2′), 4.91 (1H, d, $J_{5'a,5'b}$=10.2 Hz, H-5′b), 5.35 (1H, t, $J_{2',2'\text{-TBSOCH2a}}$=$J_{2',2'\text{-TBSOCH2b}}$=3.4 Hz, H-2′), 7.66 (1H, d, $J_{5\text{-CH3},6}$=1.1 Hz, H-6), 9.63 (1H, br, NH); ^{13}C NMR ($CDCl_3$) δ 12.6, 20.6, 23.7, 62.3, 75.5, 94.2, 102.8, 109.7, 135.8, 150.2, 164.5, 170.2; FABMS (*m*/*z*) 285 (M^++H). FABHRMS (*m*/*z*): calcd for $C_{12}H_{17}N_2O_6$: 285.1087, found: 285.1063 (M^++H).

4.14. *r*-2-Acetoxymethyl-*t*-4-methyl-*c*-4-(N^4-acetylcytosin-1-yl)-1,3-dioxolane (21β)

To a solution of **18**β (291.7 mg, 0.85 mmol) in THF (25.0 mL) was added tetrabutylammonium fluoride (1 M THF solution) (1.3 mL, 1.28 mmol) at rt under Ar atmosphere and the reaction mixture was stirred for 4.0 h. To the reaction mixture was added Ac_2O (0.65 mL, 6.83 mmol) and the mixture was stirred for 16 h. The reaction mixture was partitioned between CH_2Cl_2/saturated $NaHCO_3$ and silica gel column chromatography (dichloromethane/methanol=50:1) of the organic layer gave **21**β (239.4 mg, 90%) as a foam: UV (MeOH) λ_{max} 297 nm (ε 5600), 246 nm (ε 13,200) and λ_{min} 272 nm (ε 3100), 223 nm (ε 8400); ^{1}H NMR ($CDCl_3$) δ 1.80 (3H, s, CH_3-4′), 2.03 and 2.26 (6H, each as s, Ac), 4.02 (1H, d, $J_{5'a,5'b}$=10.4 Hz, H-5′a), 4.15 (1H, dd, $J_{2',2'\text{-TBSOCH2a}}$=3.2 Hz and $J_{2'\text{-TBSOCH2a},2'\text{-TBSOCH2b}}$=12.4 Hz, TBSO$CH_{2a}$-2′), 4.32 (1H, dd, $J_{2',2'\text{-TBSOCH2b}}$=3.4 Hz and $J_{2'\text{-TBSOCH2a},2'\text{-TBSOCH2b}}$=12.4 Hz, TBSO$CH_{2b}$-2′), 4.91 (1H, d, $J_{5'a,5'b}$=10.4 Hz, H-5′b), 5.34 (1H, dd, $J_{2',2'\text{-TBSOCH2a}}$=3.2 Hz and $J_{2',2'\text{-TBSOCH2b}}$=3.4 Hz, H-2′), 7.44 (1H, d, $J_{5,6}$=7.8 Hz, H-5), 8.21 (1H, d, $J_{5,6}$=7.8 Hz, H-6), 10.30 (1H, br, NH); ^{13}C NMR ($CDCl_3$) δ 20.6, 23.5, 24.7, 62.3, 75.0, 95.0, 96.3, 102.8, 144.7, 154.8, 163.2, 170.2, 171.1; FABMS (*m*/*z*) 312 (M^++H). Anal. Calcd for $C_{13}H_{17}N_3O_6 \cdot 3/4CH_3OH$: C, 49.25; H, 5.34; N, 12.53. Found: C, 49.10; H, 5.46; N, 12.43.

4.15. *r*-2-Hydroxymethyl-*t*-4-methyl-*c*-4-(uracil-1-yl)-1,3-dioxolane (22β)

To a solution of **19**β (192.0 mg, 3.21 mmol) in MeOH (13.0 mL) was added Et_3N (1.5 mL, 10.66 mmol) at rt under Ar atmosphere and the reaction mixture was stirred for 6 days. The reaction mixture was evaporated to dryness and silica gel column chromatography (dichloromethane/methanol=100:1) of the residue gave **22**β (153.3 mg, 95%) as a foam: UV (MeOH) λ_{max} 263 nm (ε 10,300) and λ_{min} 232 nm (ε 2300); ^{1}H NMR (DMSO-d_6) δ 1.65 (3H, s, CH_3-4′), 3.50 (2H, dd, $J_{2',2'\text{-TBSOCH2}}$=3.7 Hz and $J_{2',2'\text{-TBSOCH2OH}}$=6.1 Hz, HO$CH_2$-2′), 3.92 (1H, $J_{5'a,5'b}$=9.8 Hz, H-5′a), 4.64 (1H, d, $J_{5'a,5'b}$=9.8 Hz, H-5′b), 5.09 (1H, t, $J_{2'\text{-HOCH2a},2'\text{-HOCH2}}$=$J_{2'\text{-HOCH2b},2'\text{-HOCH2}}$=6.1 Hz, *HO*$CH_2$-2′), 5.14 (1H, t, $J_{2',2'\text{-HOOCH2a}}$=$J_{2',2'\text{-HOCH2b}}$=3.7 Hz, H-2′), 5.55 (1H, d, $J_{5,6}$=8.3 Hz, H-5), 7.92 (1H, d, $J_{5,6}$=8.3 Hz, H-6), 11.30 (1H, br, NH); ^{13}C NMR ($CDCl_3$) δ 23.4, 61.1, 74.7, 93.6, 100.5, 105.7, 140.6, 150.5, 163.8; FABMS (*m*/*z*) 229 (M^++H). Anal. Calcd for $C_9H_{12}N_2O_5$: C, 47.37; H, 5.30; N, 12.28. Found: C, 47.45; H, 5.37; N, 11.95.

4.16. *r*-2-Hydroxymethyl-*t*-4-methyl-*c*-4-(thymin-1-yl)-1,3-dioxolane (23β)

To a solution of **20**β (117.4 mg, 0.41 mmol) in MeOH (8.0 mL) was added Et_3N (0.9 mL, 6.19 mmol) at rt under Ar atmosphere and the reaction mixture was stirred for 6 days. The reaction mixture was evaporated to dryness and silica gel column chromatography (dichloromethane/methanol=100:1) of the residue gave **23**β (96.1 mg, 96%) as a foam: UV (MeOH) λ_{max} 269 nm (ε 10,300) and λ_{min} 235 nm (ε 2400); ^{1}H NMR (DMSO-d_6) δ 1.64 (3H, s, CH_3-4′), 1.77 (3H, d, $J_{CH3\text{-}5,6}$=1.1 Hz, CH_3-5), 3.51 (2H, t, $J_{2',2'\text{-HOCH2}}$=$J_{2'\text{-HOCH2},2'\text{-HOCH2}}$=6.3 Hz, HO$CH_2$-2′), 3.91 (1H, d, $J_{5'a,5'b}$=9.8 Hz, H-5′a), 4.62 (1H, d, $J_{5'a,5'b}$=9.8 Hz, H-5′b), 5.10–5.15 (2H, m, H-2′ and *HO*CH_2-2′), 7.79 (1H, d, $J_{CH3\text{-}5,6}$=1.1 Hz, H-6), 11.29 (1H, br, NH); ^{13}C NMR ($CDCl_3$) δ 12.5, 24.2, 61.8, 75.6, 93.7, 104.6, 108.8, 135.4, 150.4, 164.4; FABMS (*m*/*z*) 243 (M^++H). Anal. Calcd for $C_{10}H_{14}N_2O_5 \cdot 35/18H_2O$: C, 43.32; H, 5.09; N, 10.10. Found: C, 43.71; H, 5.27; N, 9.81.

4.17. *r*-2-Hydroxymethyl-*t*-4-methyl-*c*-4-(cytosin-1-yl)-1,3-dioxolane (24β)

To a solution of **21**β (239.4 mg, 0.77 mmol) in MeOH (15.0 mL) was added Et_3N (1.6 mL, 11.54 mmol) at rt under Ar atmosphere and the reaction mixture was stirred for 5 days. The reaction mixture was evaporated to dryness and silica gel column chromatography (dichloromethane/methanol=20:1) of the residue gave **24**β (164.3 mg, 94%) as a foam: UV (MeOH) λ_{max} 273 nm (ε 8400) and λ_{min} 252 nm (ε 6000); ^{1}H NMR (DMSO-d_6) δ 1.63 (3H, s, CH_3-4′), 3.46 (2H, dd, $J_{2',2'\text{-HOCH2}}$=3.9 Hz and $J_{2'\text{-HOCH2},2'\text{-HOCH2}}$=6.1 Hz, HO$CH_2$-2′), 3.91 (1H, d, $J_{5'a,5'b}$=9.6 Hz, H-5′a), 4.60 (1H, d, $J_{5'a,5'b}$=9.6 Hz, H-5′b), 5.04 (1H, t, $J_{2'\text{-HOCH2},2'\text{-HOCH2}}$=6.1 Hz, *HO*$CH_2$-2′), 5.12 (1H, t, $J_{2',2'\text{-HOCH2}}$=3.9 Hz, H-2′), 5.67 (1H, d, $J_{5,6}$=7.5 Hz, H-5), 7.07 (2H, br, NH_2), 7.88 (1H, d, $J_{5,6}$=7.5 Hz, H-6); ^{13}C NMR (DMSO-d_6) δ 23.8, 61.5, 74.7, 93.1, 93.3, 105.3, 141.1, 155.1, 166.2; FABMS (*m*/*z*) 228 (M^++H). Anal. Calcd for $C_9H_{13}N_3O_4 \cdot 1/8H_2O$: C, 47.43; H, 5.89; N, 18.18. Found: C, 47.52; H, 5.89; N, 17.78.

4.18. *r*-2-Hydroxymethyl-*c*-4-methyl-*t*-4-(uracil-1-yl)-1,3-dioxolane (22α)

To a solution of **16**α (212.5 mg, 0.62 mmol) in THF (18.0 mL) was added tetrabutylammonium fluoride (1 M THF solution) (0.9 mL, 0.9 mmol) at rt under Ar atmosphere and the reaction mixture was stirred for 2.0 h. To the reaction mixture was added Ac_2O (0.09 mL, 0.93 mmol) and the mixture was stirred for 16 h. The reaction mixture was partitioned between CH_2Cl_2/saturated $NaHCO_3$ and silica gel column chromatography (dichloromethane/methanol=80:1) of the organic layer gave the respective 5′-*O*-acetate (111.0 mg, 66%, foam). To a solution of the respective 5′-*O*-acetate in MeOH (8.0 mL) was added Et_3N (0.9 mL, 6.22 mmol) at rt under Ar atmosphere and the reaction mixture was stirred for 7 days. The

reaction mixture was evaporated to dryness and silica gel column chromatography (dichloromethane/methanol=50:1) of the residue gave **22α** (81.8 mg, 87%) as a foam: UV (MeOH) λ_{max} 263 nm (ε 10,300) and λ_{min} 231 nm (ε 2200); ^{1}H NMR (DMSO-d_6) δ 1.61 (3H, s, CH_3-4′), 3.53 (2H, d, $J_{2',2'\text{-HOCH2}}$=3.7 Hz, HOCH_2-5′), 4.17 (1H, d, $J_{5'a,5'b}$=9.6 Hz, H-5′a), 4.25 (1H, d, $J_{5'a,5'b}$=9.6 Hz, H-5′b), 5.01 (1H, t, $J_{2',2'\text{-HOCH2}}$=3.7 Hz, H-2′), 5.60 (1H, d, $J_{5,6}$=8.0 Hz, H-5), 7.76 (1H, d, $J_{5,6}$=8.0 Hz, H-6), 11.34 (1H, br, NH); ^{13}C NMR ($CDCl_3$) δ 24.2, 61.7, 75.5, 93.9, 101.2, 104.6, 139.8, 150.6, 163.8; FABMS (*m*/*z*) 229 (M^++H). Anal. Calcd for $C_{15}H_{26}N_2O_5$: C, 47.37; H, 5.30; N, 12.28. Found: C, 47.23; H, 5.26; N, 11.95.

4.19. *r*-2-Hydroxymethyl-*c*-4-methyl-*t*-4-(thymin-1-yl)-1,3-dioxolane (23α)

To a solution of **17α** (337.4 mg, 0.95 mmol) in THF (28.0 mL) was added tetrabutylammonium fluoride (1 M THF solution) (1.4 mL, 1.42 mmol) at rt under Ar atmosphere and the reaction mixture was stirred for 2.0 h. To the reaction mixture was added Ac_2O (0.13 mL, 1.42 mmol) and the mixture was stirred for 3.5 days. The reaction mixture was partitioned between CH_2Cl_2/saturated $NaHCO_3$ and silica gel column chromatography (dichloromethane/methanol=100:1) of the organic layer gave the respective 5′-*O*-acetate (199.2 mg, 74%, foam). To a solution of the 5′-*O*-acetate in MeOH (5.0 mL) was added Et_3N (0.63 mL, 4.54 mmol) at rt under Ar atmosphere and the reaction mixture was stirred for 7 days. The reaction mixture was evaporated to dryness and silica gel column chromatography (dichloromethane/methanol=80:1) of the residue gave **23α** (78.5 mg, 97%) as a foam: UV (MeOH) λ_{max} 268 nm (ε 10,100) and λ_{min} 235 nm (ε 2300); ^{1}H NMR (DMSO-d_3) δ 1.59 (3H, s, CH_3-4′), 1.79 (3H, s, $J_{5\text{-CH3},6}$=1.1 Hz, CH_3-5), 3.53 (2H, dd, $J_{2',2'\text{-HOCH2}}$=3.6 Hz and $J_{2'\text{-HOCH2},2'\text{-HOCH2}}$=6.0 Hz, HO$CH_2$-2′), 4.17 (1H, d, $J_{5'a,5'b}$=9.6 Hz, H-5′a), 4.24 (1H, d, $J_{5'a,5'b}$=9.6 Hz, H-5′b), 5.02–5.06 (2H, m, H-2′ and *HO*CH_2-2′), 7.63 (1H, d, $J_{5\text{-CH3},6}$=1.1 Hz, H-6), 11.30 (1H, br, NH); ^{13}C NMR ($CDCl_3$) δ 12.5, 24.1, 61.8, 75.6, 93.6, 104.5, 108.7, 135.4, 150.4, 164.4; FABMS (*m*/*z*) 243 (M^++H). Anal. Calcd for $C_{10}H_{14}N_2O_5 \cdot 1/4CH_3OH$: C, 49.19; H, 6.04; N, 11.19. Found: C, 49.42; H, 5.90; N, 10.88.

4.20. *r*-2-Hydroxymethyl-*c*-4-methyl-*t*-4-(cytosin-1-yl)-1,3-dioxolane (24α)

To a solution of **18α** (434.6 mg, 1.27 mmol) in THF (7.4 mL) was added tetrabutylammonium fluoride (1 M THF solution) (1.9 mL, 1.91 mmol) at rt under Ar atmosphere and the reaction mixture was stirred for 0.5 h. To the reaction mixture was added Ac_2O (0.96 mL, 10.18 mmol) and the mixture was stirred for 16 h. The reaction mixture was partitioned between CH_2Cl_2/saturated $NaHCO_3$ and silica gel column chromatography (dichloromethane/methanol=30:1) of the organic layer gave the 5′-*O*-acetate (324.1 mg, 82%, foam). To a solution of the respective 5′-*O*-acetate in MeOH (15.0 mL) was added Et_3N (4.35 mL, 31.23 mmol) at rt under Ar atmosphere and the reaction mixture was stirred for 3 days. The reaction mixture was evaporated to dryness and silica gel column chromatography (dichloromethane/methanol=10:1) of the residue gave **24α** (231.7 mg, 98%) as a foam: UV (MeOH) λ_{max} 273 nm (ε 7800) and λ_{min} 253 nm (ε 5800); ^{1}H NMR (DMSO-d_6) δ 1.58 (3H, s, CH_3-4′), 3.52 (2H, dd, $J_{2',2'\text{-HOCH2}}$=3.8 Hz and $J_{2'\text{-HOCH2},2'\text{-HOCH2}}$=6.1 Hz, HO$CH_2$-2′), 4.15 (1H, d, $J_{5'a,5'b}$=9.5 Hz, H-5′a), 4.19 (1H, d, $J_{5'a,5'b}$=9.5 Hz, H-5′b), 4.94 (1H, t, $J_{2',2'\text{-HOCH2}}$=3.8 Hz, H-2′), 5.04 (1H, t, $J_{2'\text{-HOCH2a},2'\text{-HOCH2}}$=$J_{2'\text{-HOCH2b},2'\text{-HOCH2}}$=6.1 Hz, *HO*$CH_2$-2′), 5.72 (1H, d, $J_{5,6}$=7.3 Hz, H-5), 7.13 (2H, br, NH_2), 7.74 (1H, d, $J_{5,6}$=7.3 Hz, H-6); ^{13}C NMR (DMSO-d_6) δ 23.8, 61.5, 74.8, 93.1, 93.3, 105.3, 141.1, 155.1, 166.2; FABMS (*m*/*z*) 228 (M^++H). Anal. Calcd for $C_9H_{13}N_3O_4 \cdot 1/9H_2O$: C, 47.16; H, 5.81; N, 18.33. Found: C, 47.55; H, 5.90; N, 17.94.

4.21. Biological test method for anti-HIV-1 activity[13,14]

The activity of these nucleoside analogues against HIV-1 replication was based on the inhibition of virus-infected cytopathogenicity in MT-4 cells. Briefly, the cells (1×10^5 cells/mL) were infected with HIV-1 at a multiplicity of infection (MOI) of 0.02 and were cultured in the presence of various concentrations of the test compounds. After a 4-day incubation at 37 °C, the number of viable cells was monitored by the 3-(4,5-dimethylthiazol-2-yl)-2,5-diphenyltetrazolium bromide (MTT) method. The cytotoxicity of the compounds was evaluated in parallel with their anti-viral activity, based on the viability of mock-infected cells.

Acknowledgements

Financial supports from Japan Society for the Promotion of Science (KAKENHI No. 24590144 to K.H.) are gratefully acknowledged. The authors are also grateful to Miss Y. Odanaka and Mrs. M. Matsubayashi (Center for Instrumental Analysis, Showa University) for technical assistance with NMR, MS, and elemental analyses.

References and notes

1. *Nucleosides and Nucleotides as Antitumor and Antiviral Agents*; Chu, C. K., Baker, D. C., Eds.; Plenum: New York, NY, 1993.
2. Ichikawa, E.; Kato, K. *Curr. Med. Chem.* **2001**, *8*, 385–423.
3. *Modified Nucleosides in Biochemistry, Biotechnology and Medicine*; Herdewijn, P., Ed.; Wiley-VCH: Weinheim, Germany, 2008.
4. Norbeck, D. W.; Spanton, S.; Broder, S.; Mitsuya, H. *Tetrahedron Lett.* **1989**, 6263–6266.
5. Kim, H. O.; Shanmuganathan, K.; Alves, A. J.; Jeong, L. S.; Beach, J. W.; Schinazi, R. F.; Chang, C.-N.; Cheng, Y.-C.; Chu, C.-K. *Tetrahedron Lett.* **1992**, *46*, 6899–6902.
6. Kim, H. O.; Ahn, S. K.; Alves, A. J.; Beach, J. W.; Jeong, L. S.; Choi, B. G.; Roey, P. V.; Schinazi, R. F.; Chu, C.-K. *J. Med. Chem.* **1992**, *35*, 1987–1995.
7. Liu, M.-C.; Luo, M.-Z.; Mozdziesz, D. E.; Lin, T.-S.; Dutschman, G. E.; Gullen, E. A.; Cheng, Y.-C.; Sartorelli, A. C. *Bioorg. Med. Chem. Lett.* **2001**, *11*, 2301–2304.
8. Bera, S.; Malik, L.; Bhat, B.; Carroll, S. S.; Hrin, R.; MacCoss, M.; McMasters, D. R.; Miller, M. D.; Moyer, G.; Olsen, D. B.; Schleif, W. A.; Tomassini, J. E.; Eldrup, A. B. *Bioorg. Med. Chem.* **2004**, *12*, 6237–6247.
9. Cappellacci, L.; Barboni, G.; Palmeieri, M.; Pasqualini, M.; Grifantini, M.; Costa, B.; Martini, C.; Franchetti, P. *J. Med. Chem.* **2002**, *45*, 1196–1202.
10. Haraguchi, K.; Takahashi, H.; Tanaka, H.; Hayakawa, H.; Ashida, N.; Nitanda, N.; Baba, M. *Bioorg. Med. Chem.* **2004**, *14*, 5309–5316.
11. Haraguchi, K.; Itoh, Y.; Tanaka, H. *J. Synth. Org. Chem. Jpn.* **2003**, *61*, 974.
12. Kubota, Y.; Kunikata, M.; Ishizaki, N.; Haraguchi, K.; Odanaka, Y.; Tanaka, H. *Tetrahedron* **2008**, *64*, 2391.
13. Baba, M.; DeClercq, E.; Tanaka, H.; Ubasawa, M.; Takashima, H.; Sekiya, K.; Nitta, I.; Umezu, K.; Nakashima, H.; Mori, S.; Shigeta, S.; Walker, R. T.; Miyasaka, T. *Proc. Natl. Acad. Sci. U.S.A.* **1991**, *88*, 2356–2360.
14. Pauwels, R.; Balzarini, J.; Baba, M.; Snoeck, R.; Schols, D.; Herdewijn, P.; Desmyster, J.; De Clercq, E. *J. Virol. Methods* **1988**, *20*, 309–312.
15. el Kouni, M. H.; Naguib, F. N. M.; Panzica, R. P.; Otter, B. A.; Chu, S.-H.; Gosselin, G.; Chu, C. K.; Schinazi, R. F.; Shealy, Y. F.; Goudgaon, N.; Ozerov, A. A.; Ueda, T.; Iltzsch, M. H. *Biochem. Pharmacol.* **1996**, *51*, 1687–1700.
16. Paterson, I.; Delgado, O.; Florence, G. J.; Lyothier, L.; O'Brein, M.; Scott, J. P.; Sereinig, N. *J. Org. Chem.* **2005**, *70*, 150–160.
17. Camps, F.; Gasol, V.; Guerrero, A. *Synthesis* **1987**, 511–512.

AAC
Journals.ASM.org

KAY-2-41, a Novel Nucleoside Analogue Inhibitor of Orthopoxviruses *In Vitro* and *In Vivo*

Sophie Duraffour,[a]* Robert Drillien,[b] Kazuhiro Haraguchi,[c] Jan Balzarini,[a] Dimitri Topalis,[a] Joost J. van den Oord,[d] Graciela Andrei,[a] Robert Snoeck[a]

Laboratory of Virology and Chemotherapy, Rega Institute for Medical Research, KU Leuven, Leuven, Belgium[a]; Institut de Génétique et de Biologie Moléculaire et Cellulaire, CNRS UMR 7104, INSERM U964, Université de Strasbourg, Strasbourg, France[b]; Nihon Pharmaceutical University, Saitama, Japan[c]; Laboratory of Translational Cell and Tissue Research, University Hospitals Leuven, Leuven, Belgium[d]

The availability of adequate treatments for poxvirus infections would be valuable not only for human use but also for veterinary use. In the search for novel antiviral agents, a 1′-methyl-substituted 4′-thiothymidine nucleoside, designated KAY-2-41, emerged as an efficient inhibitor of poxviruses. *In vitro*, KAY-2-41 was active in the micromolar range against orthopoxviruses (OPVs) and against the parapoxvirus orf. The compound preserved its antiviral potency against OPVs resistant to the reference molecule cidofovir. KAY-2-41 had no noticeable toxicity on confluent monolayers, but a cytostatic effect was seen on growing cells. Genotyping of vaccinia virus (VACV), cowpox virus, and camelpox virus selected for resistance to KAY-2-41 revealed a nucleotide deletion(s) close to the ATP binding site or a nucleotide substitution close to the substrate binding site in the viral thymidine kinase (TK; *J2R*) gene. These mutations resulted in low levels of resistance to KAY-2-41 ranging from 2.7- to 6.0-fold and cross-resistance to 5-bromo-2′-deoxyuridine (5-BrdU) but not to cidofovir. The antiviral effect of KAY-2-41 relied, at least in part, on activation (phosphorylation) by the viral TK, as shown through enzymatic assays. The compound protected animals from disease and mortality after a lethal challenge with VACV, reduced viral loads in the serum, and abolished virus replication in tissues. In conclusion, KAY-2-41 is a promising nucleoside analogue for the treatment of poxvirus-induced diseases. Our findings warrant the evaluation of additional 1′-carbon-substituted 4′-thiothymidine derivatives as broad-spectrum antiviral agents, since this molecule also showed antiviral potency against herpes simplex virus 1 in earlier studies.

Poxviruses are large double-stranded DNA viruses. Over the few last years, zoonotic orthopoxvirus (OPV) outbreaks have been widely reported, and they involved cowpox virus (CPXV), vaccinia virus (VACV), buffalopox virus, and monkeypox virus in, respectively, European countries (1), Brazil (2), India (3), and the Democratic Republic of the Congo (4). Also, orf disease, caused by the parapoxvirus orf, is a zoonosis that can be transmitted to humans by contact with infected ruminants (5, 6). Poxviruses also include the virus molluscum contagiosum, an obligate human pathogen which generally causes benign infections (7, 8). With the exception of monkeypox, which leads to generalized clinical symptoms with a life-threatening outcome, cowpox, vaccinia, orf, and molluscum contagiosum diseases are usually localized and self-limited in immunocompetent individuals. Clinical presentation can, however, be more severe when the immune status of the patient is impaired (9–12).

The access to antiviral therapies may be critical to manage such infections. There is so far no FDA- or EMA-approved drug for the treatment of poxvirus-induced diseases. Three compounds are, however, promising and have received investigational new drug status (IND) for emergency use. Among them, cidofovir {(*S*)-1-[3-hydroxy-2-(phosphonomethoxy)propyl]cytosine [(*S*)-HPMPC]; Vistide} and its prodrug, CMX001 [hexadecyloxypropyl-(*S*)-HPMPC (HDP-cidofovir)], are acyclic nucleoside phosphonates (ANPs). They are broad-spectrum antiviral molecules inhibiting poxviruses at the level of viral DNA replication by interacting with the viral DNA polymerase (E9L) (13, 14). Various studies have demonstrated their potency in inhibiting virus replication and resolving OPV-associated diseases (13–16). Cidofovir requires intravenous administration and can be nephrotoxic (13), whereas CMX001, which may be taken orally, displays some gastrointestinal toxicity (17, 18). Other ANPs containing a 2,4-diaminopyrimidine base moiety {(*R*)-9-[3-hydroxy-2-(phosphonomethoxy)propoxy]-2,4-diaminopyrimidine [(*R*)-HPMPO-DAPy]} or a 5-azacytosine base moiety {1-(*S*)-[3-hydroxy-2-(phosphonomethoxy)propyl]-5-azacytosine [(*S*)-HPMP-5-azaC]} appear to be promising for further antiviral development on the basis of their anti-OPV activities in infected cells and in animal models of poxvirus infections (19, 20). 4-Trifluoromethyl-*N*-(3,3*a*,4,4*a*,5,5*a*,6,6*a*-octahydro-1,3-dioxo-4,6-ethenocycloprop[*f*]isoindol-2(1*H*)-yl)-benzamide (ST-246) is an OPV-specific inhibitor with a distinct mode of action that targets the viral protein F13L and, as a consequence, inhibits the egress of the virus from cells (21, 22). Orally active, this compound has undergone phase 2 clinical development to assess safety, tolerability, and pharmacokinetics (23).

Nucleoside analogues are also extensively studied as therapeutic agents against the proliferation of cancer cells, against virus replication, and, recently, also against bacterial infections (24). Among them, the 2′-deoxy-4′-thiopyrimidine nucleosides have been reported to be inhibitors of some herpesviruses, and they are

Received 29 July 2013 **Returned for modification** 3 September 2013
Accepted 3 October 2013
Published ahead of print 14 October 2013
Address correspondence to Sophie Duraffour, sophie.duraffour@rega.kuleuven.be.
* Present address: Sophie Duraffour, Laboratory of Virology and Chemotherapy, Rega Institute for Medical Research, KU Leuven, Leuven, Belgium.

doi:10.1128/AAC.01601-13

TABLE 1 Overview of 2′-deoxy-4′-thiopyrimidine compounds synthesized since 1991 and evaluated as potential antiviral agents

Compound family	Compound	Antiviral activity (EC_{50} [μM])[a]	IC_{50} (μM)[b]	CC_{50} (μM)[b,c]	Reference(s)
2′-Deoxy-4′-thiopyrimidine	4′-Thiothymidine	Activity against HSV-1 (0.8) and HCMV (21)	≥32 (MRC5 cells)	2.0 (MRC5 cells)	25
	2′-Deoxy-4′-thiocytidine	No activity against HSV-1 or HCMV		1.2 (L1210 cells)	
	2′-Deoxy-4′-thiouridine	No activity against HSV-1 or HCMV		2.7 (L1210 cells)	
2′-Deoxy-4′-thionucleoside	4′-Thiothymidine	Activity against alphaherpesviruses (HSV-1, 0.37; HSV-2, 2.3; VZV, 10) and HCMV (0.98)		7.1 (Vero cells)	26
	3′-Azido-4′-thiothymidine	No activity against alphaherpesviruses (>100)		>100 (Vero cells)	
	(*E*)-5-(2-Bromovinyl)-4′-thio-2′-deoxyuridine (4′-*S*-BVDU)	Activity against alphaherpesviruses (HSV-1, 0.6; HSV-2, 10; VZV, 0.08)		>500 (Vero cells)	
5-Substituted-2′-deoxy-4′-thiopyrimidine	2′-Deoxy-5-ethyl-4′-thiouridine	Activity against alphaherpesviruses (HSV-1, 0.33; HSV-2, 3.5; VZV, 0.99); no activity against HCMV (138)		>500 (Vero cells)	28
	Other 5-substituted derivatives, including 5-propyl, 5-isopropyl, 5-cyclopropyl, and 5-(2-chloroethyl) derivatives and the molecule 4′-thio-5-vinyluridine	Active against HSV-1 (range, 0.15 to 6.8) and VZV (range, 0.3 to 4.1)		Range, >100 to >500 (Vero cells)	
1′-Carbon-substituted 2′-deoxy-4′-thiothymidine	4′-Thiothymidine	Activity against HSV-1 (0.031)	34 (HEL cells)		34
	1-(2-Deoxy-1-methyl-4-thio-β-D-ribofuranosyl)thymine (KAY-2-41)	Activity against HSV-1 (14.7); no activity against HIV-1 (>34.1)	319 (HEL cells)		
	Other derivatives of 1′-carbon-substituted 4′-thiothymidine	No activity against HSV-1 (>74) or HIV-1 (>95.1)	>367 (HEL cells)		
5-Substituted-2′-deoxy-4′-thiopyrimidine	1-(2-Deoxy-4-thio-beta-D-ribofuranosyl)-5-iodouracil (4′-thioIDU)	Activity against VACV-Cop (0.5), CPXV-BR (0.1), alphaherpesviruses (HSV-1, 0.08; HSV-2, 0.45; VZV, 2), and HCMV (5.9); no activity against HHV-6 (>100), EBV (>0.16), or HHV-8 (>4)	>100 (HFF cells)	3.0 (HFF cells)	27, 29
	4′-Thiothymidine	Activity against VACV-Cop (0.03) and CPXV-BR (0.02)	>100 (HFF cells)	<0.03 (HFF cells)	
	Other derivatives of 5-substituted-2′-deoxy-4′-thiopyrimidine	Activity against HSV-2 (range, 0.3 to 15), VACV-Cop (range, 0.03 to 0.9), and CPXV-BR (range, 0.02 to 1.6)	>88 (HFF cells)	Ranging from <0.03 to 26 (HFF cells)	

[a] HSV-1 and HSV-2, herpes simplex virus 1 and 2, respectively; VZV, varicella-zoster virus; HCMV, human cytomegalovirus; HHV-6, human herpesvirus 6; EBV, Epstein-Barr virus; HHV-8, human herpesvirus 8; HIV-1, human immunodeficiency virus type 1; VACV-Cop, vaccinia virus strain Copenhagen; CPXV-BR, cowpox virus strain Brighton.
[b] MRC-5, human lung fibroblasts; L1210, skin lymphoblast mouse cells; Vero cells, African green monkey kidney cells; HEL, human embryonic lung fibroblasts; HFF, human foreskin fibroblasts.
[c] Measured by 3-(4,5-dimethyl-2-thiazolyl)-2,5-diphenyl-2H-tetrazolium bromide assay as the inhibitory dose required to reduce the viability of the cells by 50%.

listed in Table 1 (25, 26). In particular, 4′-thiothymidine was active against herpes simplex virus 1 (HSV-1) and human cytomegalovirus (HCMV) (25), but its inhibitory activity against VACV was masked by its cytostatic effect (27). In 2003, a series of 5-substituted 2′-deoxy-4′-thiopyrimidine nucleosides was also shown to retain good antiviral activity against some herpesviruses, with the 2′-deoxy-5-ethyl-4′-thiouridine derivative being the most potent against alphaherpesviruses (28). The antiviral efficacy of 5-substituted 4′-thiopyrimidine against alphaherpesviruses and OPVs was reported in two studies (27, 29). The compound 5-iodo-4′-thio-2′-deoxyuridine (4′-thioIDU) inhibited both VACV and CPXV replication at concentrations in the nanomolar range (27).

The inhibitory activity of such molecules may rely on an initial activation step by a nucleoside kinase, such as thymidine kinase (TK), which can be of cellular or viral origin. Herpesviruses encode a type I TK, active as a homodimer, whereas OPVs encode a type II TK (the *J2R* gene in VACV strain Copenhagen [VACV-Cop]) that is (i) active as a homotetramer and (ii) homologous to the cellular cytosolic TK (human cytosolic thymidine kinase [hTK1]). These enzymes differ significantly in their substrate specificities, ranging from broad for type I TK to narrow for type II TK, with only thymidine, 2′-deoxyuridine, and closely related analogues being preferentially phosphorylated (30, 31). OPVs also encode a thymidylate kinase (TMPK; *A48R* gene) preferentially involved in the phosphorylation of the monophosphate form of thymidine to its diphosphate form (32, 33).

Therapeutic agents with novel modes of action, potent and broad antiviral activity, and good pharmacokinetic properties are still needed to enlarge the pipeline of antipoxvirus agents and to mitigate the hazard of drug resistance. In 2004, a series of 1′-carbon-substituted 4′-thiothymidines was synthesized (34), and some molecules exhibiting inhibitory activity against HSV-1 replication (Table 1) were also evaluated in preliminary assays for their activity against poxviruses (our unpublished data). One particularly active compound, 1-(2-deoxy-1-methyl-4-thio-β-D-ribofuranosyl)thymine (KAY-2-41) (Fig. 1), has now been further studied, and we describe herein the antiviral efficacy of this 4′-thiothymidine derivative against poxvirus replication in cell culture and the benefit of KAY-2-41 treatment in a VACV lethal mouse model. The antiviral activity of KAY-2-41 against ANP-resistant OPVs and the genotypic characterization of three OPVs selected for resistance to KAY-2-41 enabled us to investigate its mode of action.

MATERIALS AND METHODS

Cells. Human embryonic lung (HEL) fibroblast cells were grown in Earle's minimum essential medium (Earle's MEM; Life Technologies, Merel-

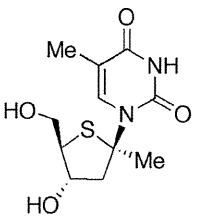

FIG 1 Structure of KAY-2-41 [1-(2-deoxy-1-methyl-4-thio-β-D-ribofuranosyl)thymine]. Me, methyl.

beke, Belgium) containing 5% fetal calf serum (FCS) and supplemented as described previously (35). Cytosolic thymidine kinase-negative human osteosarcoma cells (H143B, ATCC CRL-8303) were grown in Dulbecco's modified Eagle medium (DMEM; Life Technologies) supplemented with 10% FCS. For virus infection, the percentage of FCS for all media was reduced to 2%.

Viruses. The following virus strains were used: VACV strain Western Reserve (VACV-WR); VACV-Cop; VACV strain Lister (VACV-Lis); two VACV strains with a deletion of the *J2R* gene encoding thymidine kinase (VACV-Cop-ΔTK and VACV-WR-ΔTK); CPXV strain Brighton (CPXV-BR); various CPXV clinical isolates, including CPXV-AUS1999-867, CPXV-FIN2000-MAN, CPXV-GER1980-EP4, and CPXV-GER1991-3 (for the origins of the clinical isolates, see reference 36), kindly provided by H. Meyer (Bundeswehr Institute of Microbiology, Munich, Germany); camelpox virus (CMLV) strain Iran (CML1) and CMLV strain Dubai (CML14), kindly provided by H. Meyer (37, 38); the parapoxvirus orf strain NZ2 (ORFV-NZ2); drug-resistant VACV-WR, CML1, and CML14 harboring single or double amino acid substitutions within the *E9L* gene that result in resistance to cidofovir and/or (*S*)-1-(3-hydroxy-2-phosphonomethoxypropyl)-2,6-diaminopurine [(*S*)-HPMPDAP] (35); and VACV-WR with deletions of both ribonucleotide reductase subunits (the I4L large subunit and the F4L small subunit) (39).

Compounds. The sources of the compounds were as follow: KAY-2-41 was synthesized and characterized at Showa University, Tokyo, Japan, as described in reference 34; cidofovir [(*S*)-HPMPC] was obtained from Gilead Sciences (Foster City, CA); CMX001 (HDP-cidofovir), (*S*)-HPMP-5-azaC, and (*S*)-HPMPDAP were synthesized by M. Krečmerová (Institute of Organic Chemistry and Biochemistry, Prague, Czech Republic); (*E*)-5-(2-bromovinyl)-2′-deoxyuridine (BVDU) was synthesized by P. Herdewijn (Rega Institute, Leuven, Belgium); 5-bromo-2′-deoxyuridine (5-BrdU) and 3′-azido-3′-deoxythymidine (AZT) were purchased from Sigma-Aldrich (Schnelldorf, Germany); and ST-246 was kindly provided by D. E. Hruby from SIGA Inc. (Corvallis, OR).

Antiviral and cytostatic assays. Antiviral and cytostatic assays were performed as previously described (35). Briefly, confluent monolayers of HEL cells (in 96-well plates) were infected at a multiplicity of infection (MOI) of 0.01 PFU/cell for 2 h. Residual virus was removed and replaced with medium containing serial dilutions of the test compounds (in duplicate). After 2 to 3 days for VACV and CPXV or 4 to 5 days for CMLV, the viral cytopathic effect (CPE) was recorded under microscopic examination after ethanol fixation and Giemsa staining of 96-well plates. Scores were attributed on a scale of from 0 to 5, with a score of 0 corresponding to no CPE and a score of 5 corresponding to a 100% CPE. The 50% effective concentration (EC_{50}) was defined as the concentration of a compound required to reduce the viral CPE by 50%. Cytostatic concentrations were determined as previously reported (40). HEL cells were seeded at a density of 3.5×10^3 cells/well (in 96-well plates), and serial dilutions of test compounds were added after 1 day. Three days later, cells were washed, trypsinized, and counted with a Beckman Coulter Counter (Analis, Suarlée, Belgium), and the concentration required to inhibit cell growth by 50% (the 50% cytostatic concentration [CC_{50}]) was calculated. The minimum cytotoxic concentration (MCC) was also recorded on confluent cell monolayers and was defined as the minimum cytotoxic concentration required to alter the cell morphology.

Selection, isolation, and genotyping of viruses resistant to KAY-2-41. The VACV-WR, CPXV-BR, and CML1 strains were repeatedly passaged in HEL cells for, respectively, 30, 21, and 44 rounds in the presence of increasing concentrations of KAY-2-41, starting at 0.2 μM. Viruses that replicated in the presence of a final concentration of 20 μM KAY-2-41 were cultured twice more in drug-free medium. Antiviral assays were performed to evaluate the resistance phenotypes of these viruses. Three clones per virus strain were isolated by plaque purification and selected for further genotyping and phenotyping. All genes cited have been named following the nomenclature for VACV-Cop genes. Sequencing of *A48R* (TMPK), *E9L* (viral DNA polymerase), *D4R* (uracil DNA glycosylase), *B1R* (Ser/Thr kinase), *F10L* (Ser/Thr kinase), and *J2R* (TK) of wild-type (WT) and drug-resistant clones was performed as follows: DNA was extracted from virus-infected HEL cells using a QIAamp DNA blood minikit (Qiagen Benelux B.V, Venlo, Netherlands) following the manufacturer's instructions. The genes *A48R*, *D4R*, *B1R*, *F10L*, and *J2R* were PCR amplified as one amplicon, and the full-length *E9L* gene was amplified as five (CMLV) or four (VACV and CPXV) overlapping amplicons using FastStart high-fidelity DNA polymerase (Roche Applied Science, Mannheim, Germany) (35). Sequencing reactions and data assembling were performed as previously reported (35).

Thymidine kinase assays. The affinity of KAY-2-41 to TKs of various origins was obtained through the measurement of the activity of purified enzymes, including hTK1, human mitochondrial thymidine kinase (hTK2), and VACV-WR TK (*J2R*). The cytotoxic concentrations, or the 50% inhibitory concentrations (IC_{50}s), were calculated as the concentrations of KAY-2-41 required to inhibit 50% of the phosphorylation of the natural radiolabeled substrate [*methyl*-^{3}H]deoxythymidine ([*methyl*-^{3}H]dThd). The assays were performed in a 50-μl reaction mixture containing 50 mM Tris-HCl, pH 8.0, 2.5 mM $MgCl_2$, 10 mM dithiothreitol, 10 mM sodium fluoride, 1 mg/ml bovine serum albumin, 2.5 mM ATP, 1 μM [*methyl*-^{3}H]dThd, and enzyme. The samples were incubated at 37°C for 30 min in the presence or absence of different concentrations (5-fold dilutions) of KAY-2-41. Aliquots of 45 μl of the reaction mixtures were spotted on Whatman DE-81 filter paper disks. The filters were washed three times for 5 min each time in 1 mM ammonium formate, once for 1 min in water, and once for 5 min in ethanol. The radioactivity was determined by scintillation counting.

***In vivo* experiments.** Animal work was approved by the KU Leuven Ethics Committee for Animal Care and Use (permit number P044-2010). Infections were performed while the mice were under anesthesia using ketamine (100 mg/kg)-xylazine (10 mg/kg) in saline, and euthanasia was done by administration of pentobarbital sodium. female NMRI mice [Rj: NMRI(Han); Elevage-Janvier, Le-Genest-St-Isle, France] 5 weeks old were used. All animal experimentations were completed in biosafety level 2 facilities. Groups were defined as uninfected (mock infected) or as VACV-WR infected. After anesthesia, mice were inoculated intranasally (i.n.) with 10 μl of phosphate-buffered saline (PBS) (uninfected) or with 10 μl of PBS containing 4,000 PFU of VACV-WR (5 μl per nostril). Treatment was given intraperitoneally (i.p.) once daily for 5 consecutive days, beginning 6 h after infection, at a concentration of 5 or 50 mg/kg of body weight of KAY-2-41 dissolved in PBS. Cohorts were then monitored for body weight, morbidity, and mortality. The reported mortality rates included both actual mortality (approximately 40% of the infected animals) and mortality due to euthanasia of animals that lost more than 30% of their body weight. To determine the extent of viral replication, five mice in the VACV-WR-infected groups that received no treatment or that received KAY-2-41 at 50 mg/kg were euthanized at day 5 postinfection (p.i.), and serum as well as lungs, liver, spleen, kidneys, and mesenteric lymph nodes were collected and processed as previously described (41). Briefly, after tissue disruption and homogenization, samples were used for virus titer and viral load determinations. The virus titers in lung, liver, spleen, and kidney tissue homogenates were determined on HEL cells. Real-time quantitative PCR (qPCR) was used to quantify viral DNA, as

TABLE 2 Cytostatic concentrations, antiviral activities, and selectivity indices of compounds against poxviruses

Compound	CC_{50} (μM)[a]	VACV-Cop		VACV-Lis		VACV-WR		CPXV-BR		CML1		ORF-NZ2	
		EC_{50} (μM)[b]	SI[c]	EC_{50} (μM)	SI	EC_{50} (μM)	SI	EC_{50} (μM)	SI	EC_{50} (μM)	SI	EC_{50} (μM)	SI
KAY-2-41	14 ± 10	0.48 ± 0.33	29	0.41 ± 0.33	34	0.80 ± 0.37	18	0.48 ± 0.15	29	0.79 ± 0.40	18	3.5 ± 0.7	4
Cidofovir	397 ± 255	6.9 ± 3.0	57	9.1 ± 6.6	44	8.2 ± 2.6	48	13.9 ± 8.3	29	11.2 ± 4.5	35	0.8 ± 0.1	496
(*S*)-HPMP-5-azaC	125 ± 79	5.5 ± 2.7	23	10.0 ± 6.3	12	7.5 ± 1.4	17	11.5 ± 4.6	11	13.3 ± 6.4	9	0.5 ± 0.1	250
CMX001	≥2.4 ± 1.8	0.005 ± 0.002	≥467	0.023 ± 0.021	≥106	0.013 ± 0.011	≥180	0.021 ± 0.026	≥114	0.024 ± 0.022	≥100	—[d]	—

[a] CC_{50}, 50% cytostatic concentration, or the drug concentration required to reduce HEL cell growth by 50%. Data represent the means ± standard deviations of at least three independent experiments.

[b] EC_{50}, 50% effective concentration, or the concentration of compound required to reduce the viral cytopathic effect by 50%. Data are shown as the means ± standard deviations of at least four independent experiments.

[c] SI, selectivity index, or the ratio CC_{50}/EC_{50}.

[d] —, not done.

previously reported (41). Organs from one mouse of each group were used for histological examination (41).

Statistical analyses. All statistical analyses were done with GraphPad Prism (version 6) software (GraphPad Software Inc., La Jolla, CA). Unpaired *t* tests were used to compare mean EC_{50}s, obtained from at least three independent experiments, between WT and drug-resistant viruses. The Mann-Whitney test, two-tailed, was used to compare the ranks of the viral DNA loads or virus titers of KAY-2-41-treated mice to those of the PBS-treated group. Statistical significance was defined for the above-described tests as follows: $P < 0.001$, extremely significant; $P < 0.01$, very significant; $P < 0.05$, significant; and $P > 0.05$, not significant (NS).

RESULTS

Antiviral activity of KAY-2-41 against poxviruses. Several 1′-carbon-substituted 4′-thiothymidines were synthesized, and due to its anti-HSV-1 activity (34), KAY-2-41 was further evaluated for its activity against poxviruses. In HEL cells, KAY-2-41 emerged as a potent inhibitor of OPVs and displayed EC_{50}s of 0.48 ± 0.33 μM against VACV-Cop, 0.48 ± 0.15 μM against CPXV-BR, and 0.79 ± 0.40 μM against CML1 (Table 2). Similar KAY-2-41 EC_{50}s were also observed with two other VACVs (VACV-Lis and VACV-WR). The compound appeared to be 10- to 15-fold more active than two nucleotide phosphonate analogues, i.e., cidofovir and (*S*)-HPMP-5-azaC, which had mean EC_{50}s of 9.8 μM and 9.6 μM, respectively, against the different OPVs. The lipid prodrug derivative of cidofovir, CMX001, was 395-fold (VACV-Lis) to 1,380-fold (VACV-Cop) more active than its parent counterpart, cidofovir, and 18-fold (VACV-Lis) to 96-fold (VACV-Cop) more active than KAY-2-41. Also, the KAY-2-41 EC_{50} against CPXV-BR was in the range of that of ST-246, yet ST-246 was 32- to 80-fold more potent against the other OPV strains.

We also examined whether KAY-2-41 was active against nonlaboratory OPV strains and assessed various CPXV clinical isolates collected from human and animal cowpox cases (36). The molecule potently inhibited CPXV-GER1991-3 (mean EC_{50}, 0.46 ± 0.21 μM), CPXV-GER1980-EP4 (mean EC_{50}, 0.28 ± 0.06 μM), CPXV-FIN2000-MAN (mean EC_{50}, 0.42 ± 0.007 μM), and CPXV-GER1999-867 (mean EC_{50}, 0.58 ± 0.22 μM).

KAY-2-41 was not found to alter the cell morphology of stationary cells (MCC value > 100 μM). The molecule was, however, cytostatic for growing HEL cells, with a CC_{50} value of 14 ± 10 μM, which accounted for the relatively low selectivity indices (SIs; ratio of CC_{50}/EC_{50}) ranging from 18 to 29 (Table 2). Similarly, the CC_{50} value of CMX001 was ≥2.4 ± 1.8 μM, but because of its potency, SIs were ≥100. The molecules cidofovir, (*S*)-HPMP-5-azaC, and ST-246 were less toxic for growing cells than KAY-2-41. Both ANPs had SIs comparable to the SI of KAY-2-41, while ST-246 was the most selective molecule with an SI of ≥1,696.

We could further demonstrate that KAY-2-41 had a 4-fold weaker activity against the parapoxvirus ORF-NZ2 than OPVs, with an EC_{50} of 3.5 ± 0.7 μM (Table 2). Both ANPs evaluated were potent inhibitors of ORF-NZ2, while ST-246 was not active, which is consistent with the specific anti-OPV activity of ST-246.

Antiviral activity of KAY-2-41 against cidofovir and (*S*)-HPMPDAP-resistant OPVs. Being a thymidine analogue, the triphosphate form of KAY-2-41 was expected to interact ultimately with the viral DNA polymerase E9L in VACV-Cop to block virus replication. We therefore wondered whether KAY-2-41 could inhibit OPVs bearing mutations within E9L that are known to confer resistance to certain ANPs. In previous studies, we identified such amino acid substitutions in the exonuclease domain of E9L (A314V), in the polymerase domain (T831I), or in both domains (A314V plus A684V) (35). Recombinant CML1, CML14, and VACV harboring these amino acid substitutions were used, and the two ANPs cidofovir and (*S*)-HPMPDAP were included as control drugs to confirm the resistance phenotype of each strain (Table 3). The presence of the A314V or the T831I substitution did not alter the sensitivity of VACV, CML1, and CML14 to KAY-2-41, while these amino acid substitutions conferred resistance to cidofovir and/or (*S*)-HPMPDAP. Interestingly, mutating both exonuclease and polymerase domains of E9L (A314V plus A684V) appeared to render CML14 and VACV even more sensitive to the effect of KAY-2-41, albeit the shifts in EC_{50}s, compared to those for the WT viruses, were only 4.6-fold (0.10 μM versus 0.46 μM [$P = 0.0164$] for CML14) and 3.85-fold (0.2 μM versus 0.77 μM [$P = 0.0173$] for VACV) (Table 3). On the other hand, the A314V and A684V substitutions were responsible for high levels of resistance to cidofovir and (*S*)-HPMPDAP. In conclusion, KAY-2-41 was endowed with potent antiviral efficacy against cidofovir-resistant viruses, and the molecule appeared to have a slightly increased activity when the A314V and A684V mutations were present.

Selection, genotyping, and phenotyping of OPVs resistant to KAY-2-41 (KAY-2-41^r). To elucidate the mode of action of KAY-2-41, drug-resistant viruses were isolated following 21 (CPXV-BR), 30 (VACV-WR), and 44 (CML1) passages in the presence of increasing amounts of the drug. Three clones of each virus stock were plaque purified and used for further analysis.

Genotypic characterization revealed the presence of a nucleotide deletion(s) and one nucleotide substitution in the TK (*J2R*)

TABLE 3 Antiviral activity of KAY-2-41 against cidofovir and (*S*)-HPMPDAP-resistant CMLV and VACV

	EC_{50} (μM)[a]								
Compound	CML14	CML14 A314V[b]	CML14 A314V + A684V[b]	CML1	CML1 T831I[b]	VACV-WR	VACV-WR A314V[b]	VACV-WR A314V + A684V[b]	VACV-WR T831I[b]
(*S*)-HPMPC	8.6 ± 3.2	24.4 ± 12.4*	49.4 ± 21.4*	7.1 ± 3.0	9.6 ± 3.6	16.7 ± 9.3	64.7 ± 30.2**	148.4 ± 23.0***	108.7 ± 42.1***
(*S*)-HPMPDAP	0.5 ± 0.1	14.6 ± 4.2***	17.4 ± 10.6*	0.2 ± 0.1	4.1 ± 2.8**	2.0 ± 1.1	17.3 ± 9.7***	53.0 ± 13.9***	31.3 ± 9.4***
KAY-2-41	0.46 ± 0.22	0.22 ± 0.11	0.10 ± 0.01*	0.29 ± 0.11	0.26 ± 0.13	0.77 ± 0.46	0.44 ± 0.24	0.20 ± 0.12*	1.09 ± 0.35

[a] EC_{50}, 50% effective concentration, or the concentration of compound required to reduce the viral cytopathic effect by 50%. Data are shown as the means ± standard deviations of at least four independent experiments. Asterisks indicate where the EC_{50} differs significantly from that of the corresponding WT virus, as determined by an unpaired *t* test: *, $P < 0.05$; **, $P < 0.01$; ***, $P < 0.001$.

[b] Drug-resistant recombinant viruses previously characterized (35) and bearing amino acid substitutions, i.e., A314V, A314V plus A684V, or T831I, in the viral DNA polymerase (E9L).

gene of each of the KAY-2-41^r clones, whereas the gene sequences of the TMPK (*A48R*), two serine/threonine kinases (*B1R* and *F10L*), the uracil DNA glycosylase (*D4R*), and the viral DNA polymerase (*E9L*) were comparable to those of the corresponding WT clones. Figure 2 depicts the mutations found in the viral TK. Resistant VACV-WR clones had a deletion of a thymine at position 43 (Tdel43) leading to a frameshift mutation from amino acid 15, changing the serine into a glutamine, until the appearance of a stop codon at position 21. CPXV-BR clones harbored a double deletion of a guanine and a thymine at positions 73 and 74 (GT-del73/74) that resulted in a stop codon at position 25. These frameshift mutations by deletions were all found in the ATP binding region, localized in the N-terminal extremity of the TK, and led to the production of truncated viral TKs. In contrast, KAY-2-41^r CML1 clones showed a substitution mutation at position 328 (G328T) that modified the aspartic acid 110 into a tyrosine (D110Y).

We further proceeded to the phenotypic characterization of the KAY-2-41^r clones. As shown in Fig. 3A to C, relatively low levels of resistance to KAY-2-41 were found for the mutant viruses, as they were only 2.7-, 6.0-, and 5.8-fold greater for VACV-WR, CPXV-BR, and CML1 KAY-2-41^r, respectively, than for their WT counterparts. These drug-resistant viruses displayed a trend in hypersensitivity toward the nucleoside analogue BVDU, while

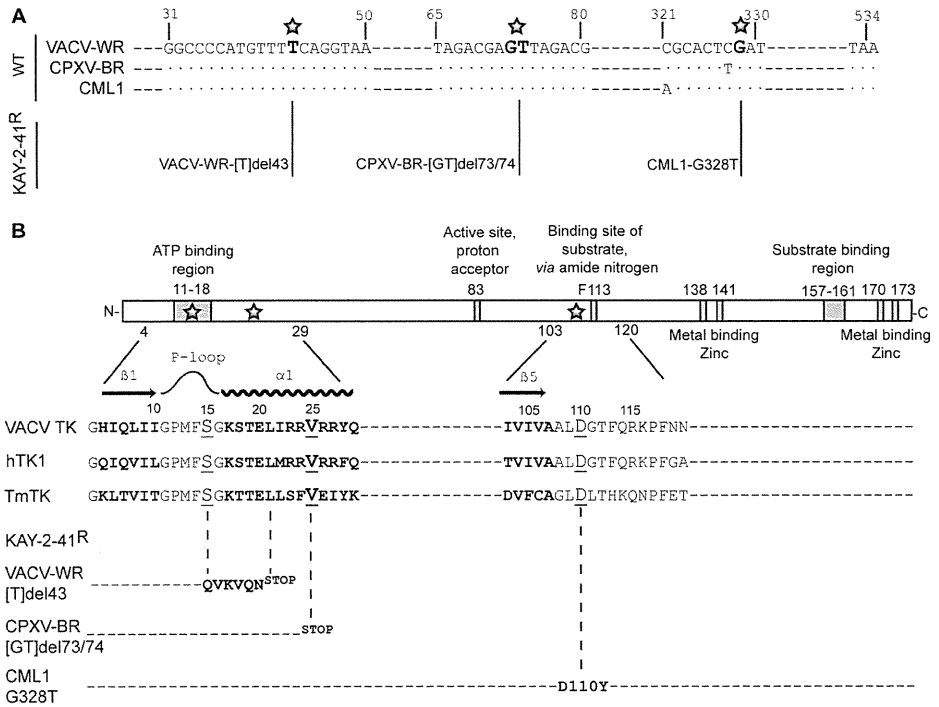

FIG 2 Mapping of mutations found in KAY-2-41^r viruses and overview of OPV thymidine kinase. (A) Nucleotide sequences of regions of the TK gene of the VACV-WR, CPXV-BR, and CML1 wild-type viruses that were found to be mutated in KAY-2-41^r viruses. The position of mutations found in KAY-2-41^r viruses are indicated in bold and with a star. The name of each resistant strain, i.e., VACV-WR-[T]del43, CPXV-BR-[GT]del73/74, and CML1-G328T, is given. (B) A schematic view of the TK protein highlighting the major regions involved in ATP, substrate, and metal binding is presented. A partial sequence of the VACV-WR TK is shown for the regions where amino acid substitutions were identified proximal to the β1 sheet-P loop-α1 helix or the β5 sheet. Protein sequences of the human cytosolic TK (hTK1) and of *Thermotoga maritima* TK (*Tm*TK) are also shown for comparison purposes. The amino acid substitutions found in KAY-2-41^r viruses are presented for each of the viruses and are represented by a star in the schematic view or by underlining in the amino acid sequences.

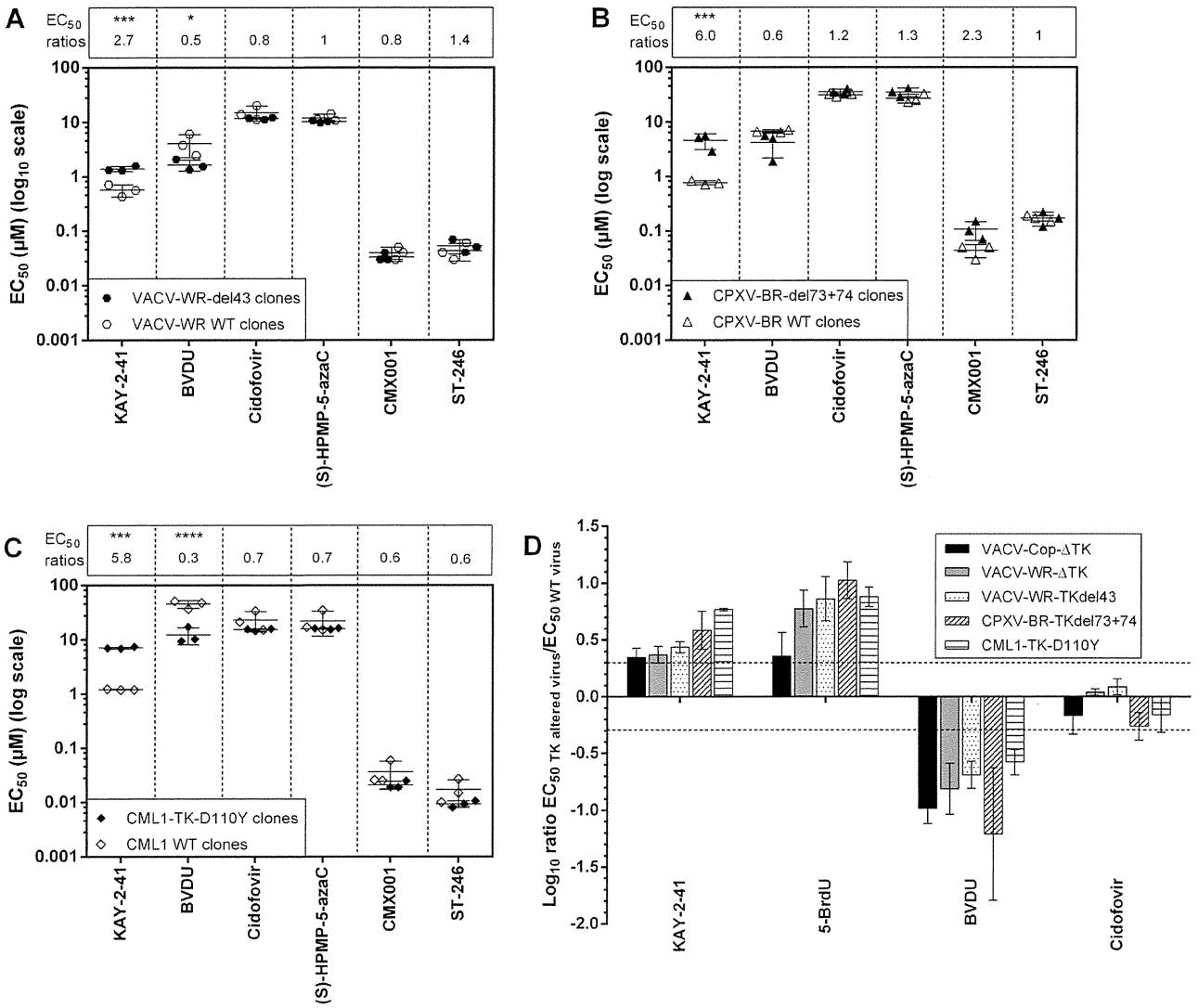

FIG 3 Drug resistance profiles of plaque-purified VACV-WR (A), CPXV-BR (B), and CML1 (C) KAY-2-41^r clones and of viruses with thymidine kinase deletions (D). (A to C) Three clones of each WT and drug-resistant virus were used for plaque reduction assays, and at least three to four independent experiments were performed for each compound tested. The data are presented as a dot plot of the EC_{50}s of the KAY-2-41^r clones (filled symbols) versus the EC_{50}s of the WT parent clones (empty symbols). On top of each graph are shown the fold changes in EC_{50}s, which were calculated as the ratio of the mean EC_{50}s of the KAY-2-41^r clones divided by the mean EC_{50}s of the WT clones. Results are presented as means ± standard deviations. The statistical significance of the differences in drug sensitivity of the resistant viruses compared to that of the WT is indicated as follows: *, $P < 0.05$; ***, $P < 0.001$; ****, $P < 0.0001$. (D) Plaque reduction assays were done with each of the three KAY-2-41^r strains, two VACV strains with TK deletions, and their corresponding WT viruses in three independent experiments. Results are plotted on a linear scale as the $\log_{10}$ of the ratios of the EC_{50}s, and standard deviations are given. Resistance was observed with a ratio of >2 (log 0.3), and hypersensitivity was observed with a ratio of <0.5 (log −0.3).

ANPs and ST-246 showed inhibitory activities in the range of those of WT viruses.

To further investigate whether mutations within the TK gene may be one of the determinants responsible for the resistance phenotype, we used two VACV strains with deletions in TK (VACV-Cop-ΔTK and VACV-WR-ΔTK) and evaluated the profiles of their sensitivities to four drugs (Fig. 3D). Viruses with TK deletions showed resistance to KAY-2-41 and to 5-BrdU, another TK-dependent drug, and hypersensitivity to BVDU, a TMPK-dependent drug, while cidofovir kept its full activity. Similar observations were made with each of the KAY-2-41^r OPVs, suggesting the requirement of viral TK in the antiviral effect of KAY-2-41. Cross-resistance to 5-BrdU reinforced this conclusion, as it partially relied on viral TK to be active. Additionally, the TK-negative phenotype of each of the KAY-2-41^r OPVs was confirmed by the ability of these viruses to multiply in H143B TK-deficient cells in the presence of a KAY-2-41 or 5-BrdU concentration which was inhibitory for the WT viruses (data not shown).

We also evaluated the potential involvement of the ribonucleotide reductase in KAY-2-41 efficacy by using a VACV-WR strain with deletions in both ribonucleotide reductase subunits, I4L and F4L. KAY-2-41 conserved its inhibitory activity against this virus with an EC_{50} of 0.97 ± 0.18 μM, which is in the range of that for the WT virus. A similar observation was made with 5-BrdU, which

TABLE 4 Inhibitory activity of KAY-2-41, 5-BrdU, AZT and BVDU on dThd phosphorylation by VACV-TK, hTK1, and hTK2

Compound	IC_{50} (μM)[a]		
	VACV TK	hTK1	hTK2
KAY-2-41	490 ± 1	≥500	352 ± 55
5-BrdU	2.9 ± 1.1	3.0 ± 0.0	3.6 ± 0.6
AZT	16 ± 0	5.8 ± 3.9	2.4 ± 0.6
BVDU	>500	>500	0.36 ± 0.05

[a] IC_{50}, 50% inhibitory concentrations, or the concentration of compound required to inhibit the binding of the natural substrate dThd by 50%. Data are shown as the means ± standard deviations of two independent experiments. VACV TK, vaccinia virus thymidine kinase; hTK1, human cytosolic thymidine kinase; hTK2, human mitochondrial thymidine kinase.

had an EC_{50} of 0.2 μM against the virus with the I4L/F4L deletion versus an EC_{50} of 0.32 μM against the WT virus.

KAY-2-41 interacts with VACV TK. Next, we wanted to know whether KAY-2-41 could alter the phosphorylating activity of VACV TK, hTK1, and hTK2 for their natural substrate. Enzymatic TK assays based on the competitive binding between the natural substrate dThd and KAY-2-41 demonstrated that KAY-2-41 was inhibitory to the phosphorylation of radiolabeled dThd by hTK2, VACV TK, and hTK1, in decreasing order of potency (Table 4). The inhibition was, however, much weaker than that observed for 5-BrdU and AZT, which appeared to be rather potent competitive inhibitors of dThd phosphorylation, with IC_{50}s ranging, respectively, from 2.9 to 3.6 μM and from 2.4 to 16 μM. In contrast, BVDU strongly affected dThd phosphorylation by hTK2, but not by VACV TK or hTK1, at the highest concentration tested (50 μM).

***In vivo* evaluation of KAY-2-41.** A mouse model of lethal VACV-WR infection was used to determine the efficacy of KAY-2-41 treatment *in vivo*. As shown in Fig. 4, all animals intranasally exposed to VACV-WR and treated with vehicle (PBS) died by day 7 p.i. In contrast, both VACV-WR-challenged cohorts that received KAY-2-41 systemically (i.p. injection) at a dose of 5 or 50 mg/kg once daily for 5 consecutive days, starting on the day of infection, survived the infection. The group of infected mice that received 5 mg/kg of the drug had a pronounced loss of body weight between days 5 and 10 p.i., but after this time point, animals progressively recovered. Among the animals receiving the 50-mg/kg treatment regimen, a slight loss of body weight was seen. The effect of a similar treatment with KAY-2-41 (50 mg/kg) was also assessed in mock-infected animals, and no apparent morbidity was observed, as evidenced by a body weight evolution comparable to that of untreated animals (Fig. 4).

On the basis of these results, we further evaluated the impact of the 50-mg/kg KAY-2-41 treatment on viral DNA loads and VACV-WR replication in various organs. Mice were infected and treated in the same way as in the first experiment. Four (VACV-WR-infected) or five (VACV-WR-infected and KAY-2-41-treated) animals per group were sacrificed at day 5 p.i. The efficacy of the compound was confirmed, as KAY-2-41 (50 mg/kg daily for 5 consecutive days) protected 100% of the animals from VACV-WR mortality, with no apparent morbidity (Fig. 5). As depicted in Fig. 5B, viral DNA was detected in all organs of infected untreated mice, with means of 5.1 (kidneys) to 6.5 (lungs) log DNA copies/g, and the sera were also positive (4.2 log DNA copies/50 μl serum) at this time point. Lung, liver, and spleen tissues showed the highest levels of viral DNA, which were equivalent to mean viral titers of, respectively, 3.8, 3.3, and 3.5 log 50% tissue culture infective doses ($TCID_{50}$s)/g. Treating the mice with KAY-2-41 significantly reduced viral DNA loads in various organs, including lungs (means, 4.0 versus 6.5 log DNA copies/g), liver (means, 1.2 versus 6.6 log DNA copies/g), spleen (means, 4.5 versus 6.3 log DNA copies/g), and serum (means, 2.5 versus 4.2 log DNA copies/g). A similar trend was also noticed in the kidneys and mesenteric lymph nodes. Viral titrations further demonstrated the absence of replicating virus in lungs, liver, spleen, and kidneys. Histological examination of the lung tissue revealed the absence of inflammation in KAY-2-41-treated animals, which, strikingly, contrasts with the interstitial inflammation seen in infected untreated animals (Fig. 5C).

DISCUSSION

To our knowledge, the *in vitro* and *in vivo* antipoxvirus activity of a 1′-carbon-substituted 4′-thiothymidine derivative has not yet been reported. Other laboratories have demonstrated the inhibitory potential of 5-substituted 4′-thiopyrimidine nucleoside derivatives against poxviruses (27, 29), despite the fact that the narrow substrate specificity of poxvirus TK remains a challenge for selecting potent nucleoside analogues. Our study demonstrated that OPVs (VACVs, CPXVs, and CML1) are efficiently inhibited by KAY-2-41 *in vitro* at concentrations in the submicromolar range. This activity was also displayed against a variety of cowpox clinical isolates, a finding which may have implications for clinical use in the current context of the increased incidence of cowpox virus infections (1, 42). KAY-2-41 appeared to be more potent than cidofovir and (*S*)-HPMP-5-azaC, albeit the prodrug of cidofovir, CMX001, and ST-246, a morphogenesis inhibitor, remained the most active molecules toward OPVs.

KAY-2-41 was effective in inhibiting the replication of mutant viruses resistant to cidofovir and/or (*S*)-HPMPDAP. If KAY-2-41 in its triphosphate metabolite form ultimately targets the viral DNA polymerase, our data suggest that the presence of the A314V or T831I mutation in the DNA polymerase gene (*E9L*) did not impact its ability to accept this substrate, whereas these changes clearly influenced the acceptance of acyclic nucleoside pyrimidine and purine analogues [i.e., cidofovir and (*S*)-HPMPDAP]. In fact,

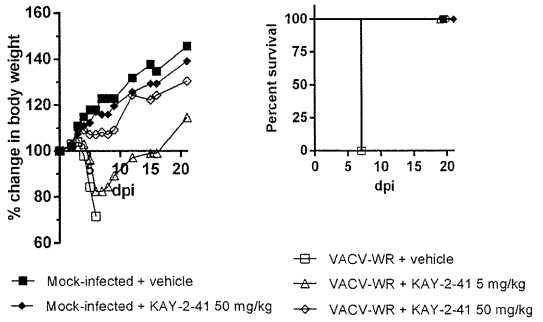

FIG 4 KAY-2-41 protects mice from VACV-WR-induced mortality. NMRI mice (5 mice per group) were challenged intranasally either with vehicle (mock infected) or with VACV-WR. Animals were then treated with PBS or with the drug at a dose of 5 or 50 mg/kg once per day for 5 consecutive days starting at 6 h after infection. Cohorts were monitored for 20 days for body weight (left) and survival (right). Body weight evolution is shown as the percentage of the change in the average weight for each group of mice.

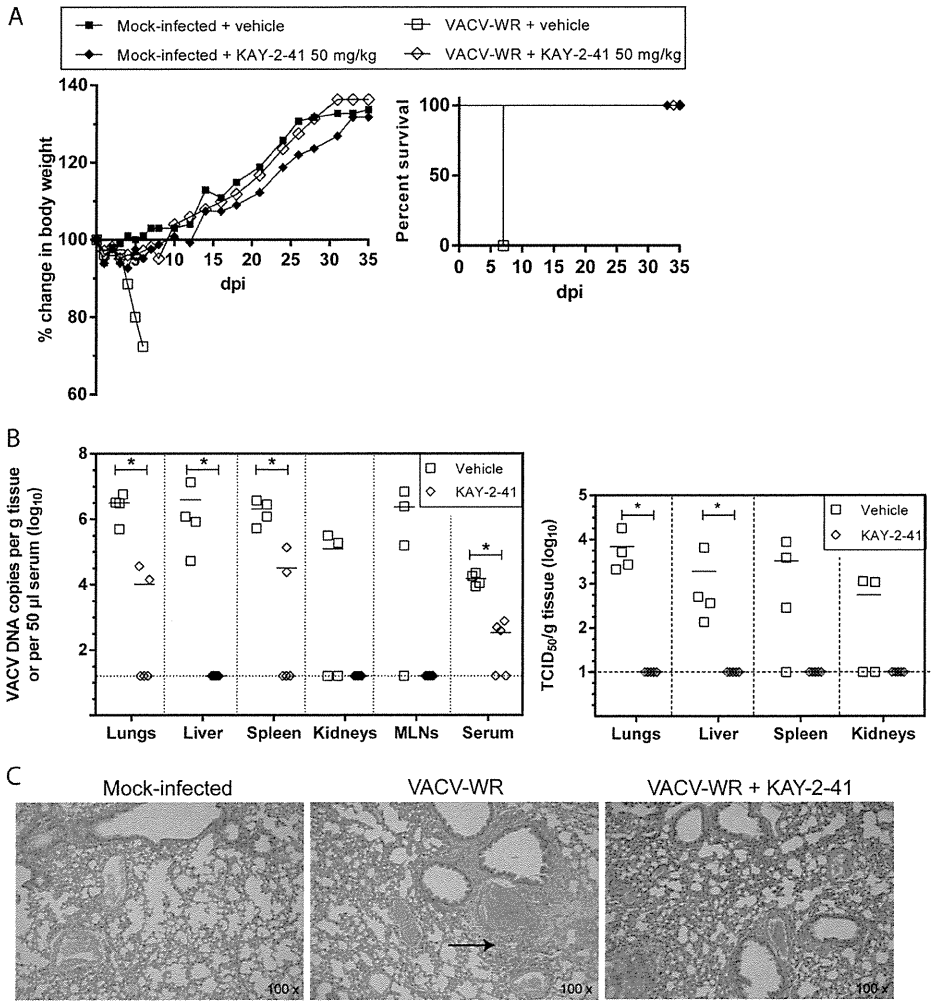

FIG 5 KAY-2-41 treatment inhibits virus dissemination and replication in various organs. (A) Body weight evolution and survival curves of mock-infected and VACV-WR-infected mice that received vehicle (PBS) or KAY-2-41 treatment at 50 mg/kg once a day for 5 consecutive days beginning 6 h after virus exposure. Body weight evolution is shown as the percentage of the change in average weight for each group of mice (5 mice per group). dpi, day postinfection. (B) Viral DNA loads in various organs and in serum (left) and virus titers in lungs, liver, spleen, and kidneys (right) are shown. Animals were sacrificed at day 5 p.i. Viral loads were determined by qPCR and are expressed as VACV DNA copy numbers per g of tissue or per 50 µl of serum. Virus titers are shown in $TCID_{50}$s per g tissue. The scatter plots show the viral DNA loads or virus titers from individual mice and the means (horizontal bars) for each group. Four (VACV-WR-infected) or five (VACV-WR-infected and KAY-2-41-treated [50 mg/kg]) individual mice were used lung. MLNs, mesenteric lymph nodes. Dashed lines, limit of detection. The viral DNA loads or virus titers of KAY-2-41-treated mice differed significantly from those of the PBS-treated group by the Mann-Whitney test (*, $P < 0.05$). (C) Lung tissue examination at 5 days p.i. While VACV-WR-treated mice exhibited interstitial inflammation (arrow), no inflammatory cells were seen after KAY-2-41 treatment.

while these mutations were associated with different ANP resistance profiles when present in a CMLV or in a VACV backbone (in line with our published observations [35]), KAY-2-41 remained equally active against WT and mutant viruses bearing the A314V or T831I mutation. Interestingly, the CML14 and VACV A314V plus A684V double mutants appeared to be more sensitive to KAY-2-41 inhibition, suggesting that through these conformational changes, E9L might become more prone to accept the thymidine analogue triphosphate metabolite.

Being a nucleoside analogue, the involvement of the viral TK was expected to be important for the metabolic activation of the molecule, and the genotypic characterization of KAY-2-41^r strains confirmed this hypothesis. Additionally, the poor but significant antiviral activity of KAY-2-41 against the parapoxvirus orf in comparison to that against OPVs was of interest, as it also pointed toward the need for TK for KAY-2-41 to inhibit OPVs. Indeed, this virus does not possess a specific TK gene (43), and in line with that, the EC_{50} against ORFV-NZ2 was in the range of the EC_{50}s seen with KAY-2-41^r viruses. Sequencing of KAY-2-41^r clones allowed us to identify mutations in the TK gene that are most likely responsible for the drug-resistant phenotype since they were identified only in drug-resistant viruses. Five other viral genes investigated, including *A48R* (TMPK), *B1R* (Ser/Thr kinase), *F10L* (Ser/Thr kinase), *E9L* (DNA polymerase), and *D4R* (uracil DNA glycosylase), had sequences that were identical to those of the corresponding WT viruses. Also, a VACV-WR mutant with a deletion in ribonucleotide reductase subunits did not display resistance to KAY-2-41 or to 5-BrdU. In contrast, two viruses with TK deletions displayed resistance to both KAY-2-41 and 5-BrdU (which are TK dependent) and not to BVDU (which is TMPK dependent), mimicking the drug resistance pheno-